



Advanced Actuators for Planetary Applications

Xiaoqi Bao, PhD

Non-Destructive Evaluation & Advanced Actuator
Jet Propulsion Laboratory, California Institute of Technology
Pasadena, CA

Presented at Seminar on Modern Actuators for Aerospace Applications

I-Shou University, Kaohsiung, Taiwan

November 24, 2003

Introduction

Actuators are a key element of space mechanisms and instruments:

- For deployment, mobility, sampling, transfer, handling, alignment, precision position control
- Need to have reduced size, mass, and power consumption, high performance and lower cost.

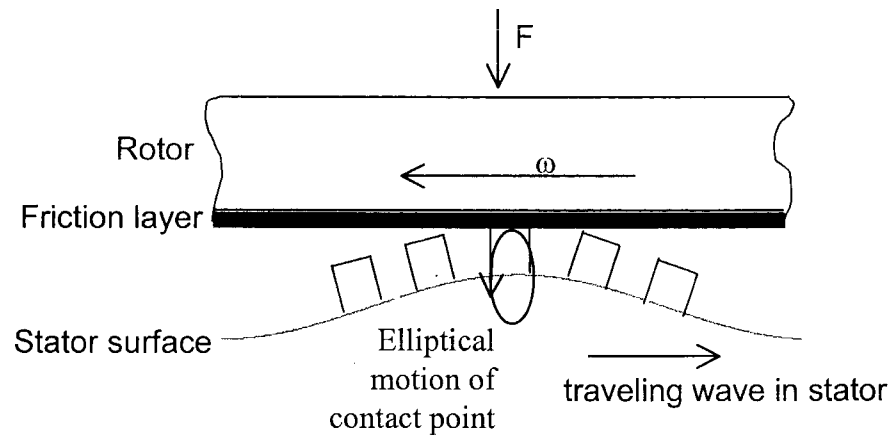
To address these needs, novel actuation mechanisms employing electroactive materials (piezoceramics and polymers) are being developed at the NDEAA Lab of JPL.

In this presentation:

- Piezoelectric ceramics&crystal actuators: ultrasonic motor, piezopump, 2-DoF surface acoustic wave motors, USDC and URAT.
- Electroactive polymer (EAP) actuators are being explored for various mechanisms ranging from dust wiper to currently exploring controlled large optics.

The actuation mechanisms analytical and numerical models will be reviewed. Also, current and potential capabilities will be discussed.

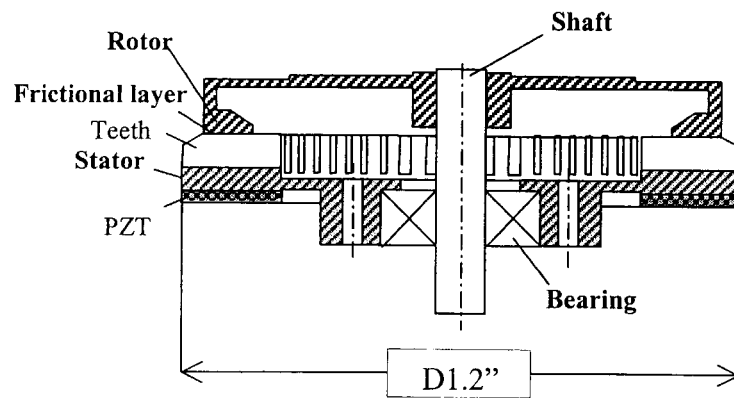
Ultrasonic Traveling Wave Motors



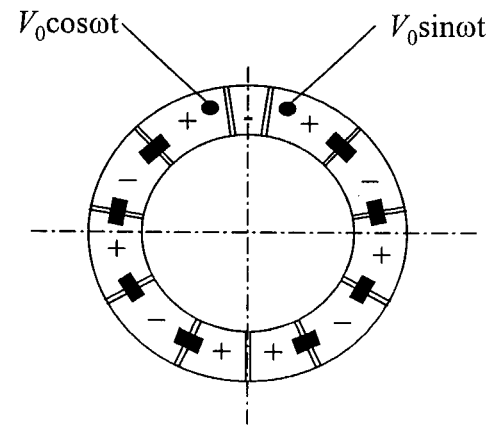
Merits:

- 1) High torque and low speed --suitable for direct drive;
- 2) Quick response, wide speed range, hard brake and no backlash
--excellent position controllability
- 3) Silent operation
- 4) Compact size and light weight
- 5) Simple structure --potential low cost.

Ultrasonic Motors



JPL prototype USM

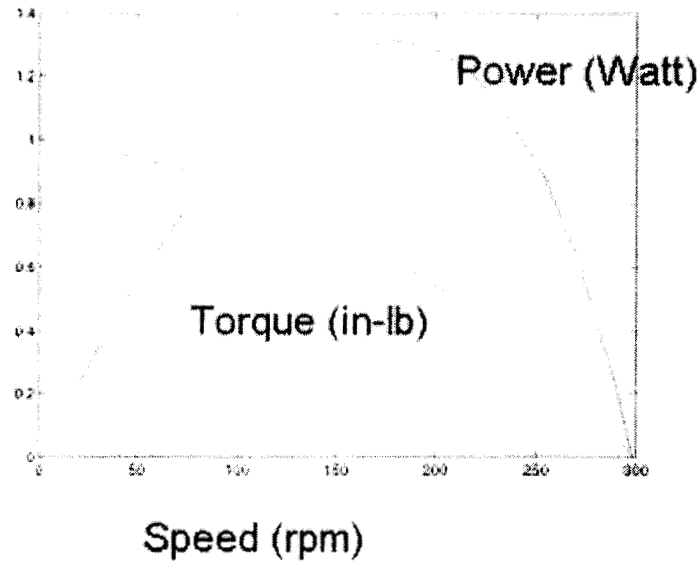
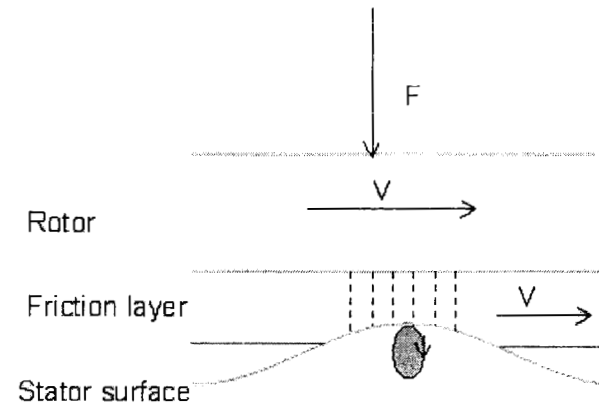


PZT ring

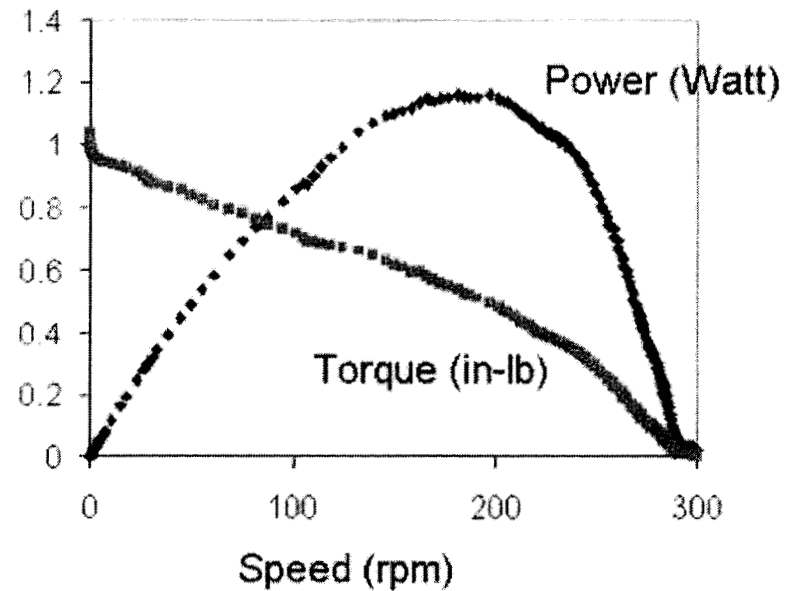
USM performance modeling

Mechanical Loading of the Stator Friction Layer and Rotor - Model assumptions

- Rigid rotor
- Friction layer as vertical springs in Z direction
- The speed in Y direction is the same as the rotor

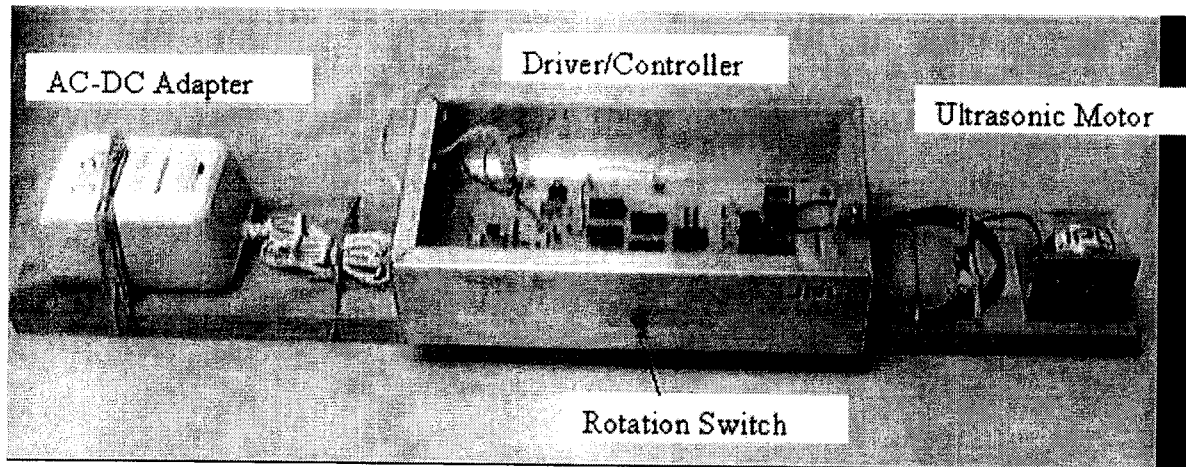


Predicted by computer model

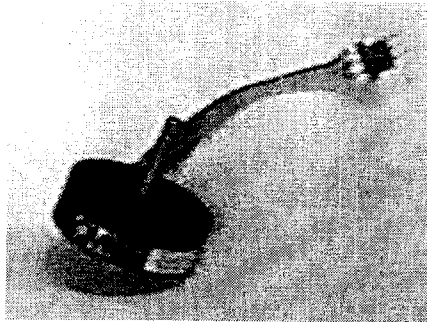


Measured performance of JPL prototype

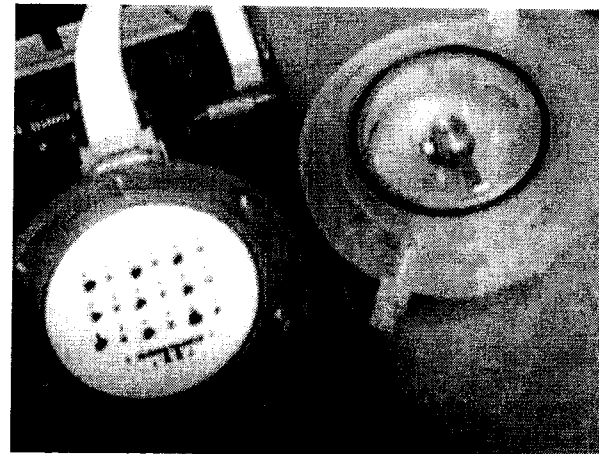
JPL USM



Demo set



JPL/QMI Prototype USM



Application for E-Tongue probe cleaning

USM's Performance

A recent effort to improve the performance of the prototype done by JPL team increased the stall torque to 1.4 inch-lb and doubled the maximum speed to 600 rpm. Correspondingly, the estimated maximum output power is increased to 3.3 W.

The estimation formulas for a scaled motor:

Torque $T \sim D^3$,

Speed(rpm) $\Omega \sim 1/D$,

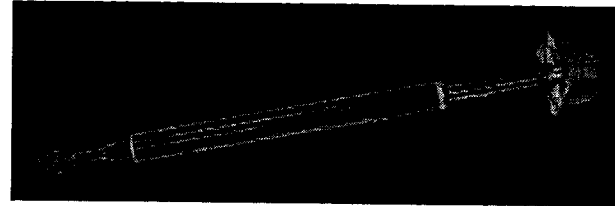
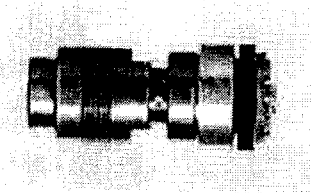
Power $W \sim D^2$

		Prototype motor	Estimation scaled motor
Sizes	Stator	D1.2"(30mm)x0.15"	D2.4"(60mm) x0.15"
	Rotor	D1.2"xD0.785x0.15"	D2.4"x0.15"
Maximum	Speed	600 rpm	300 rpm
	Torque	1.4 inch-lbs	11 inch-lbs
Loaded for maximum power	Speed	400 rpm	200 rpm
	Torque	0.7 inch-lb	5.6 inch-lbs
	Power	3.3 W	13 W

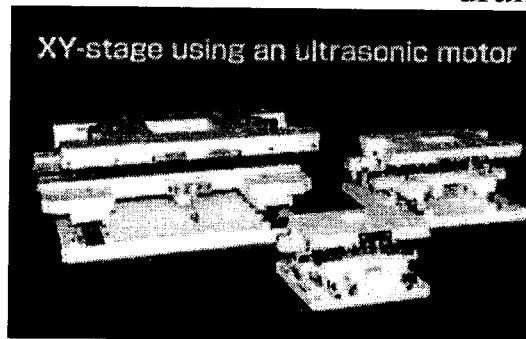
USM application



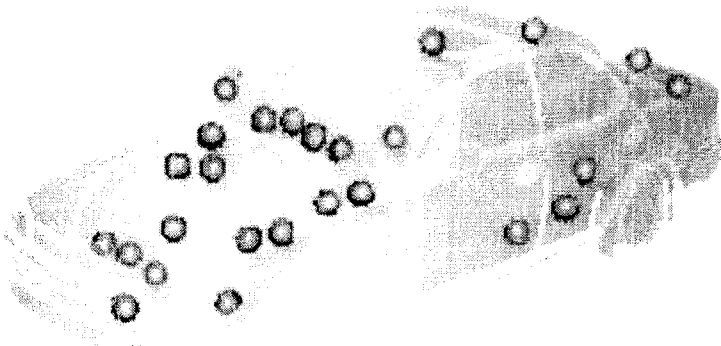
Canon lens



High-precision drive technology is the USM that drives the four photosensitive drums and the paper transfer belt.



Kyocera

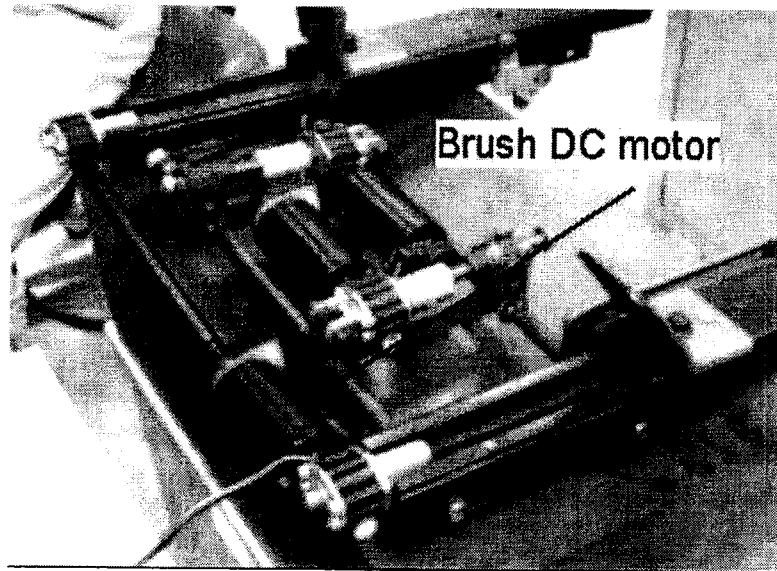


Small motors on a car



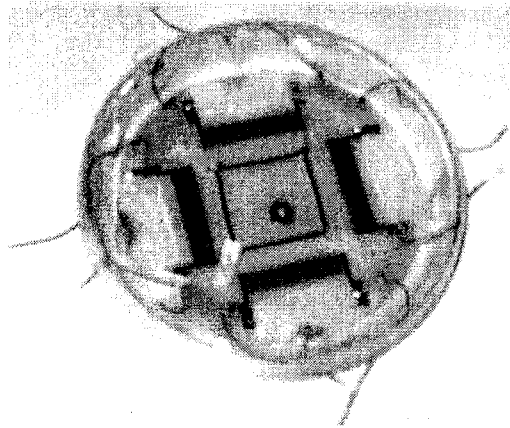
USM for driving wheel tilt

USM application

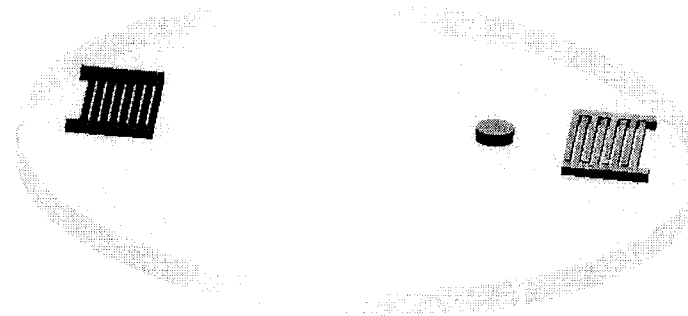


Ford was interested in USM for seat adjustment

Surface Acoustic Wave (SAW) Motors



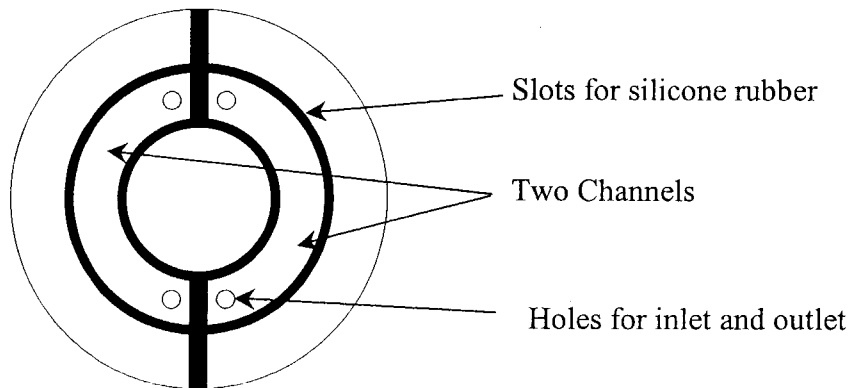
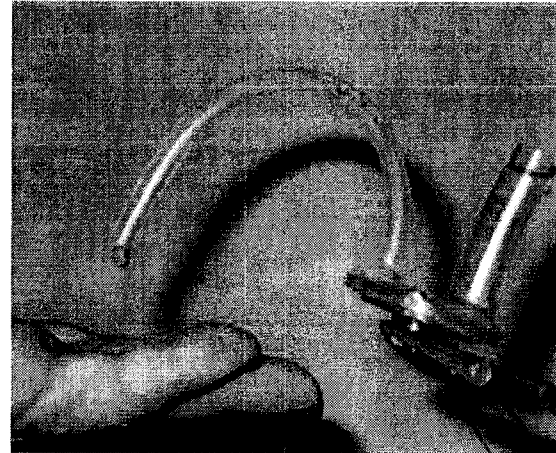
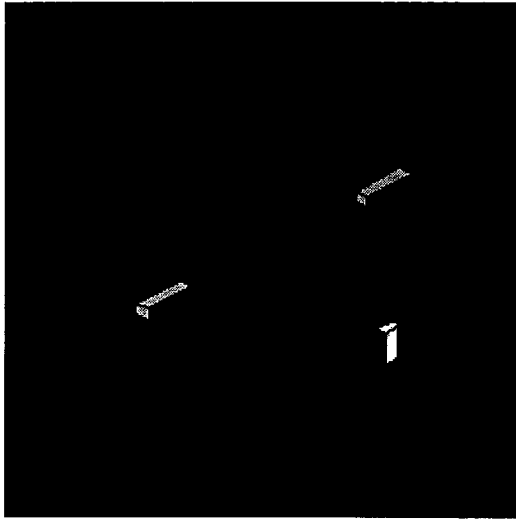
■ Signal On



IDT excite a surface wave on piezoelectric substrate
causes a mass to surf towards the source

On 128° Y-cut LiNiO_3
Velocity up to 1 m/s
40-nanometers step

Piezoelectric Pump



Top cover of the pump

Current Specifications

4-5 cc/min

1100 Pa

No Moving Parts

Peristaltic

Ultrasonic/Sonic Driller/Corer (USDC)

A tool developed for rock sample acquisition and in-situ analysis in NASA missions to Mars, Titan, comets and asteroids

- Basic configuration
 - An ultrasonic horn transducer.
 - A free flying mass (free-mass)
 - A drill stem
- Basic working principle
 - The free-mass bounces between the horn tip and a drill stem at sonic frequencies .
 - The impacts of the free-mass create stress pulses that propagate to the interface of the stem tip and the rock.
 - The rock fractures when its ultimate strain is exceeded.

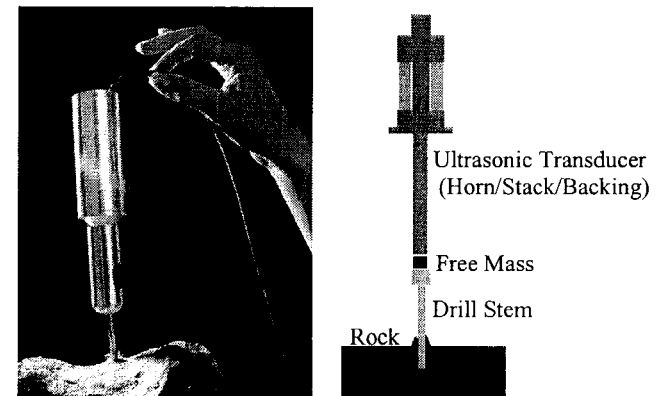
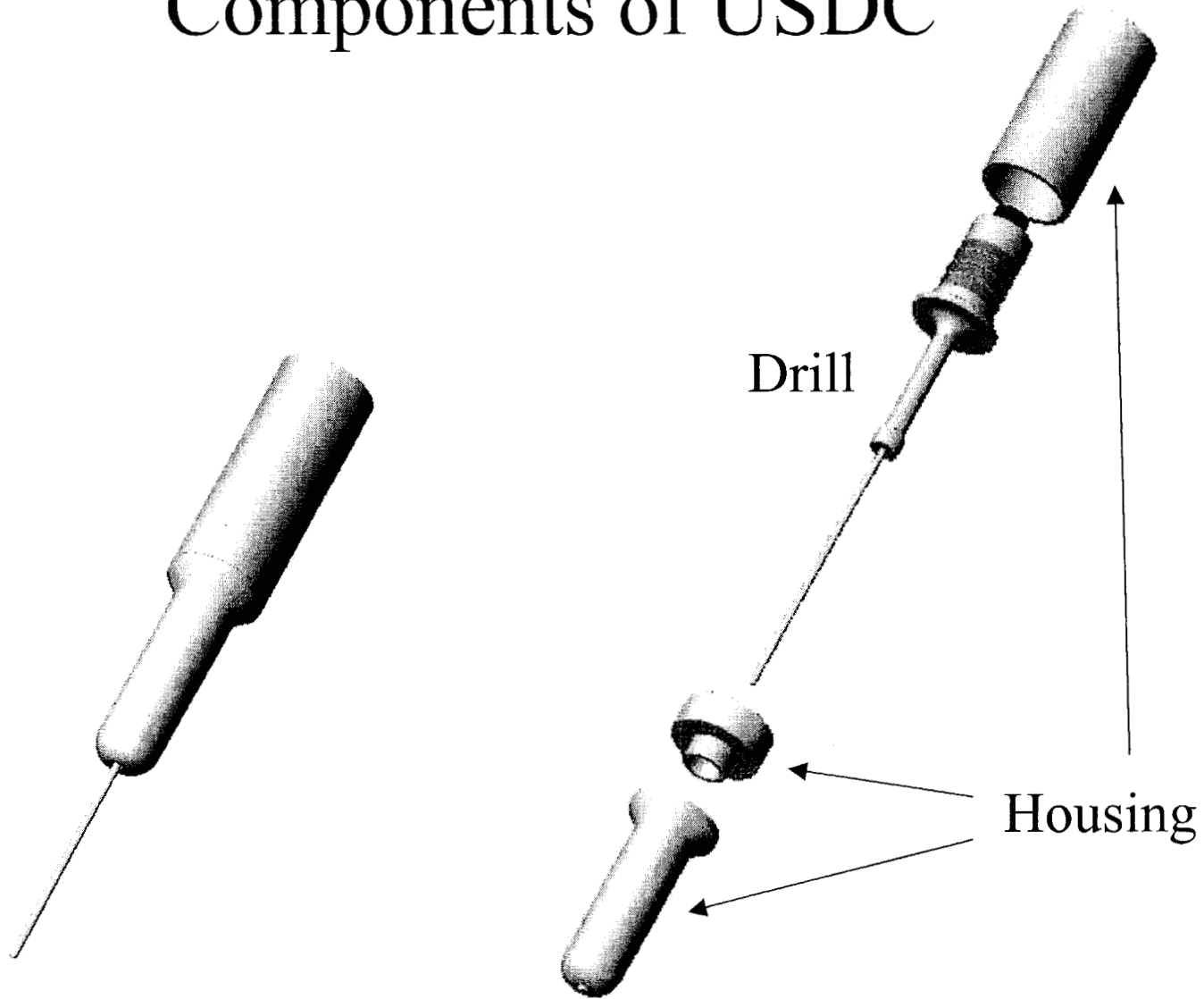


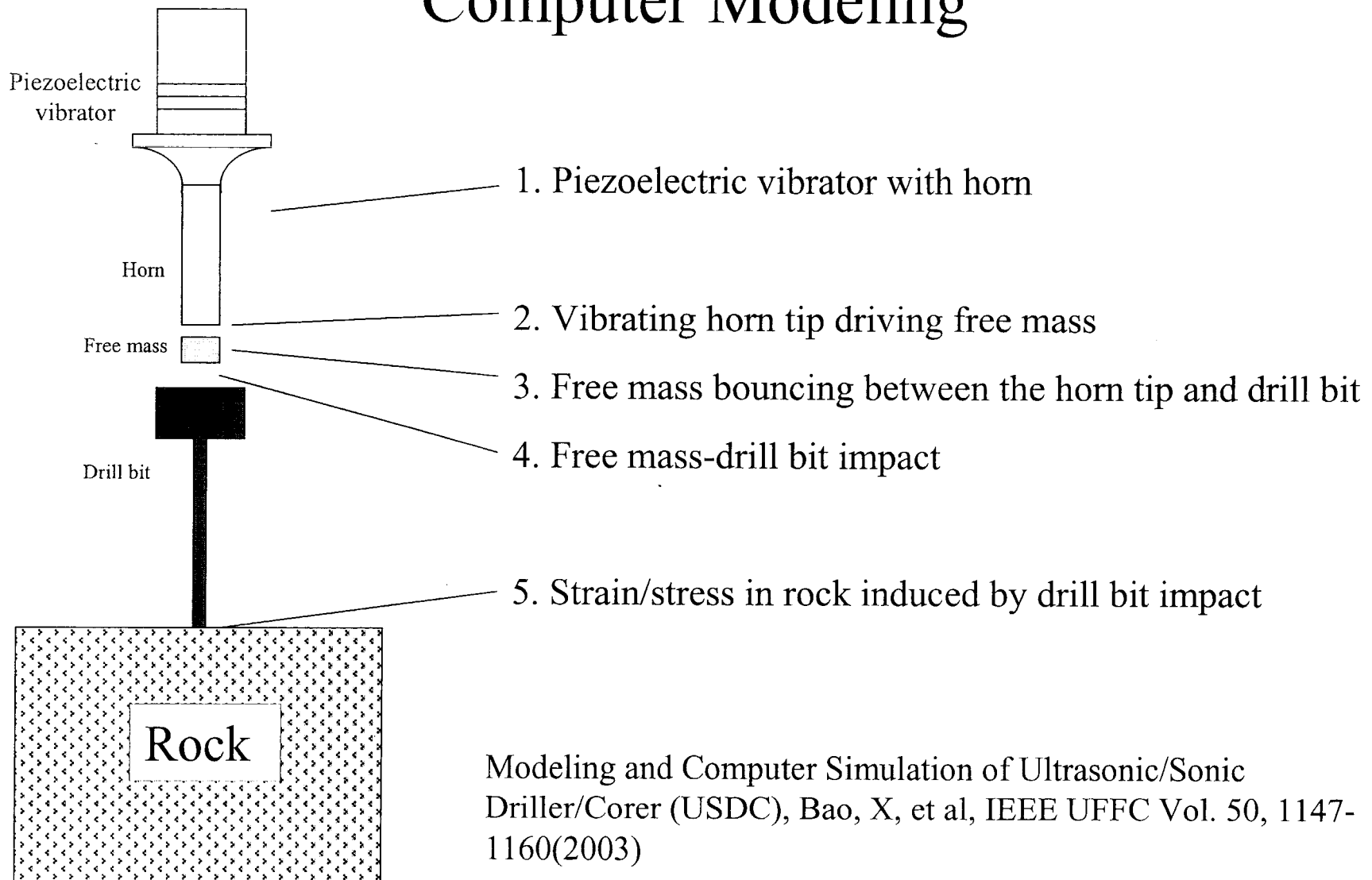
Fig. 1. The USDC is shown coring with minimum axial force and holding torque (left), and a schematic diagram of the USDC device (right).

- Features
 - Low mass and low power
 - Minimum axial load requirement
 - Near zero holding torque

Components of USDC

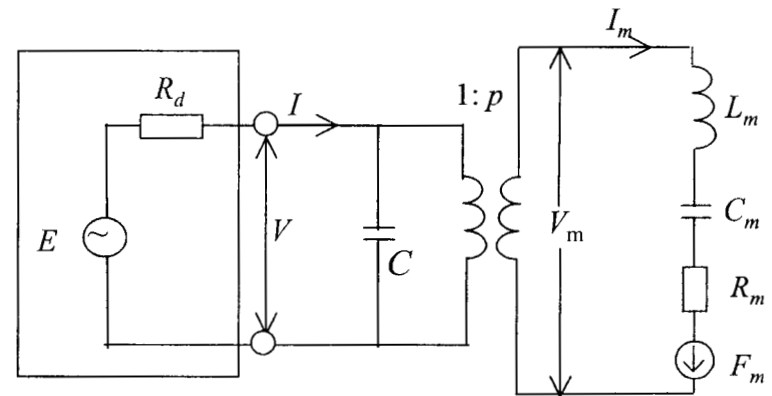
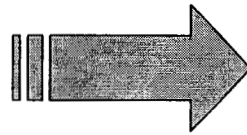
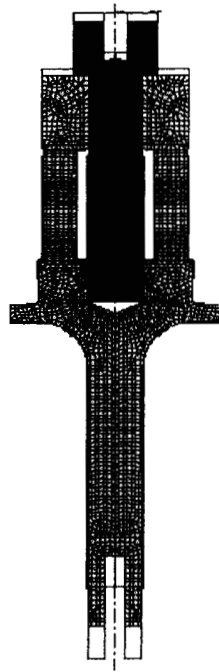


Computer Modeling



Modeling and Computer Simulation of Ultrasonic/Sonic Driller/Corer (USDC), Bao, X, et al, IEEE UFFC Vol. 50, 1147-1160(2003)

Piezoelectric transducer



FEM Modal Analysis. Figure shows calculated modal shape at resonance of 22.668 kHz. The outline is the un-deformed.

Schematic of the equivalent circuit of the transducer around resonance.

Reaction of free-mass impacts

Impact force on the tip

$$F_c = f_I \delta(t - t_I)$$

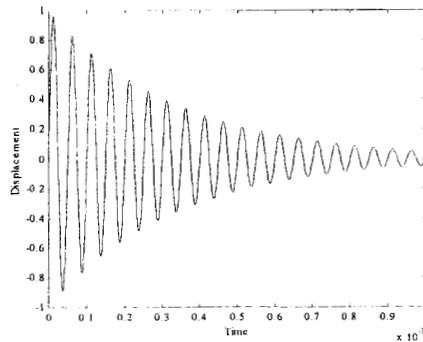
Translation velocity change

$$f_I = -m\Delta v_I$$

$$\Delta U_I = \frac{-m\Delta v_I}{M} H(t - t_I)$$

$$U = U_0 + at + \sum_I \Delta U_I$$

Induced vibration

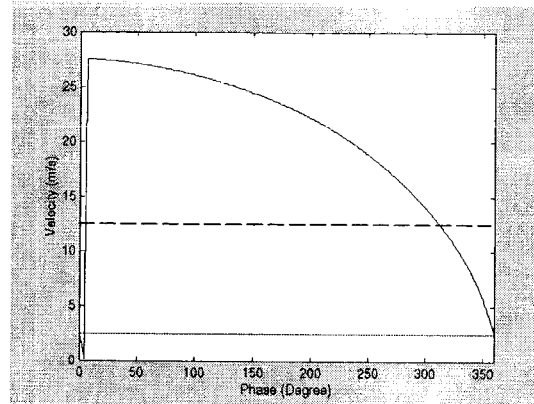
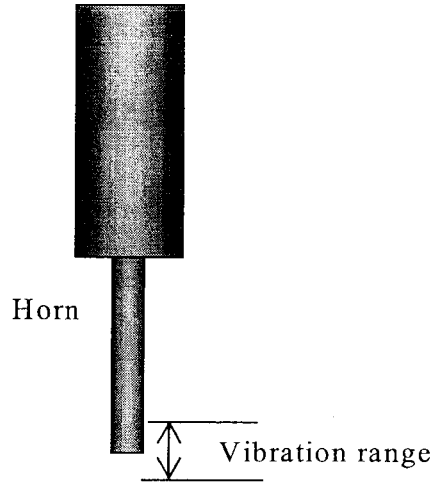


$$I_{mI} = \dot{d}_I = -\frac{m\Delta v_I \xi_I}{L_m} \exp[(-\alpha + j\omega_f)(t - t_I)]$$

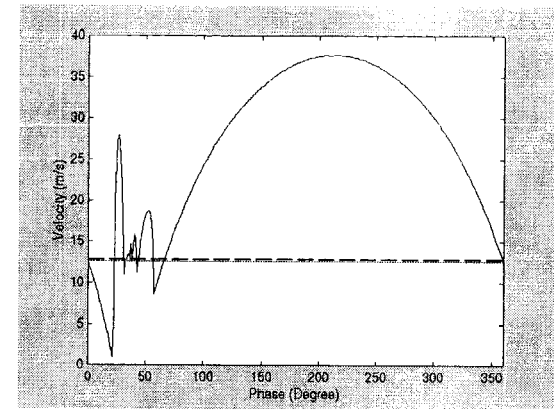
$$t > t_I$$

Free-mass Driven by Vibrating Tip

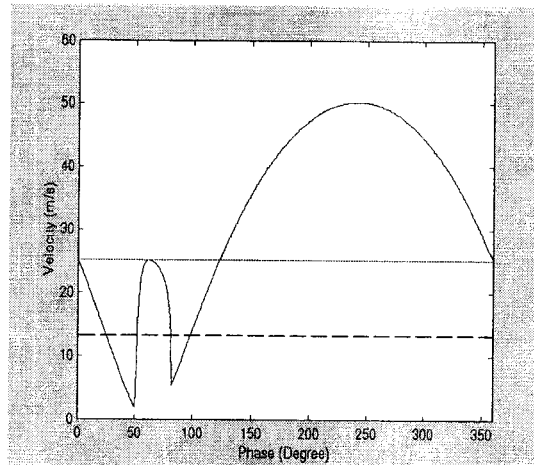
Simple collision model



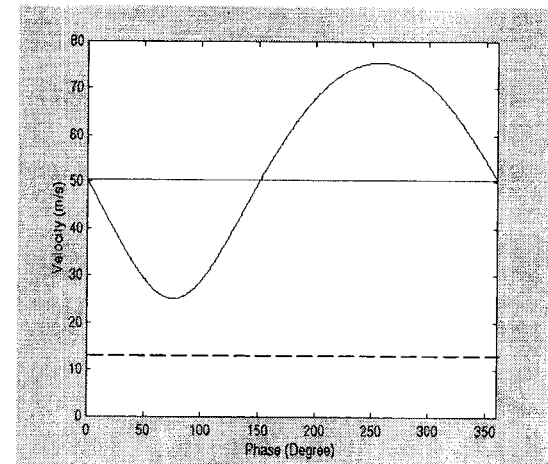
$V_{in} = 0.2 V_{tmax}$



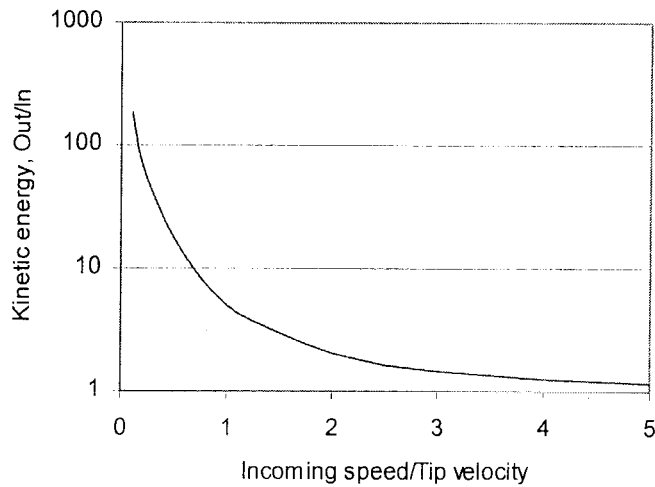
$V_{in} = 1.0 V_{tmax}$



$V_{in} = 2.0 V_{tmax}$



$V_{in} = 4.0 V_{tmax}$



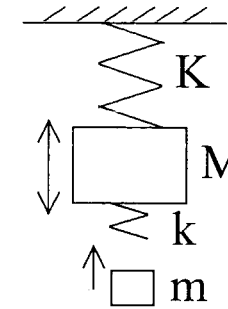
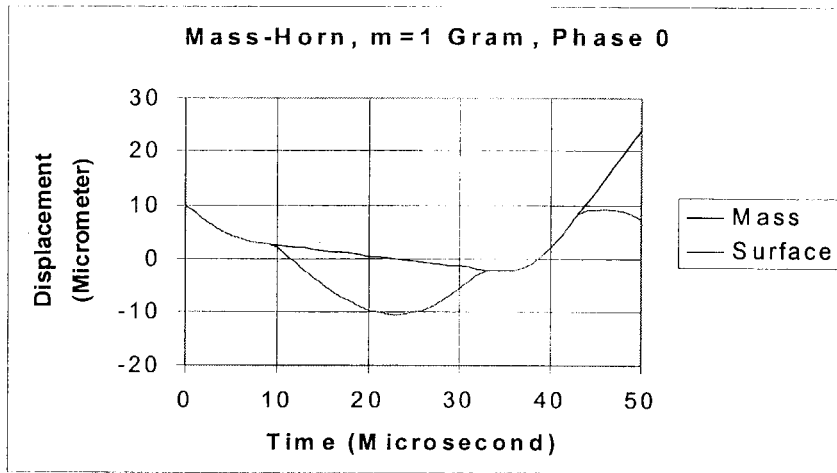
Average increase of the free-mass energy

———— indicates the free-mass coming velocity.

----- indicates the tip maximum velocity.

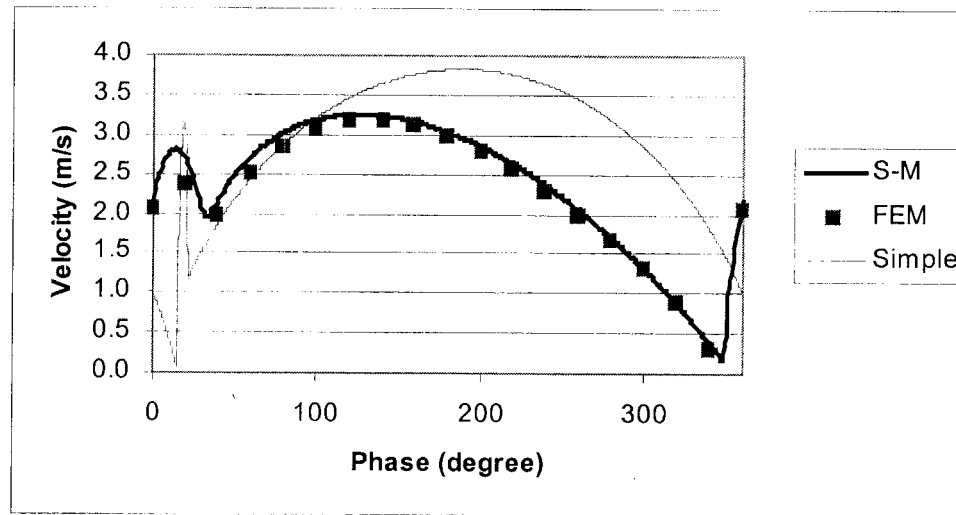
Free-mass Driven by Vibrating Tip

FEM & Spring-mass model



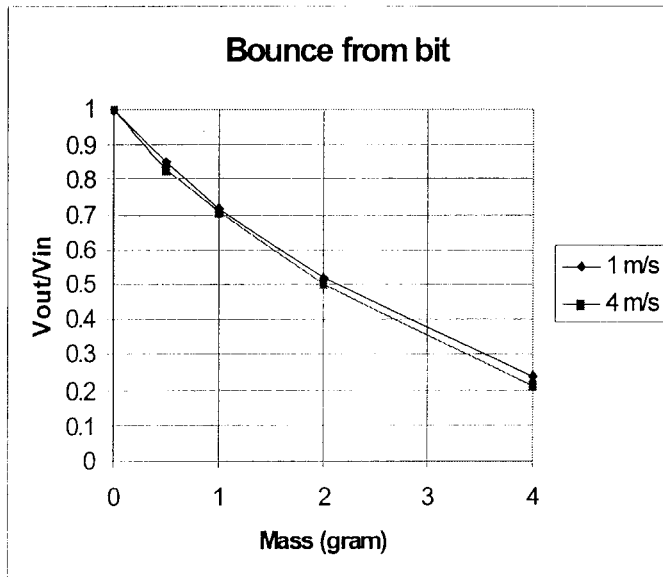
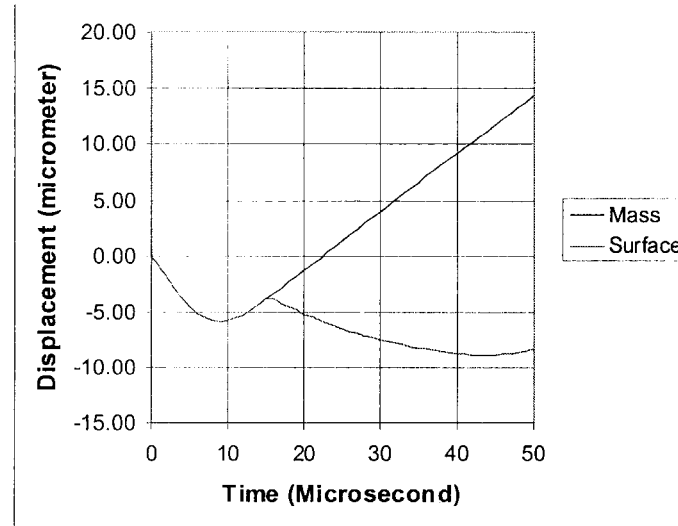
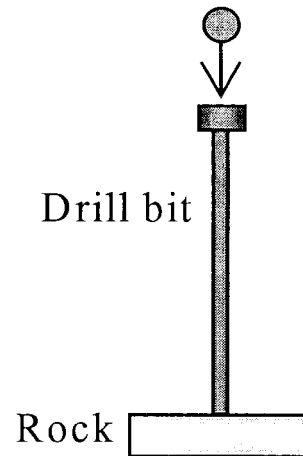
Spring-mass model

FEM: The free-mass and surface displacement as a function of the time.



Comparison of the three models

Free-mass bounce from the bit

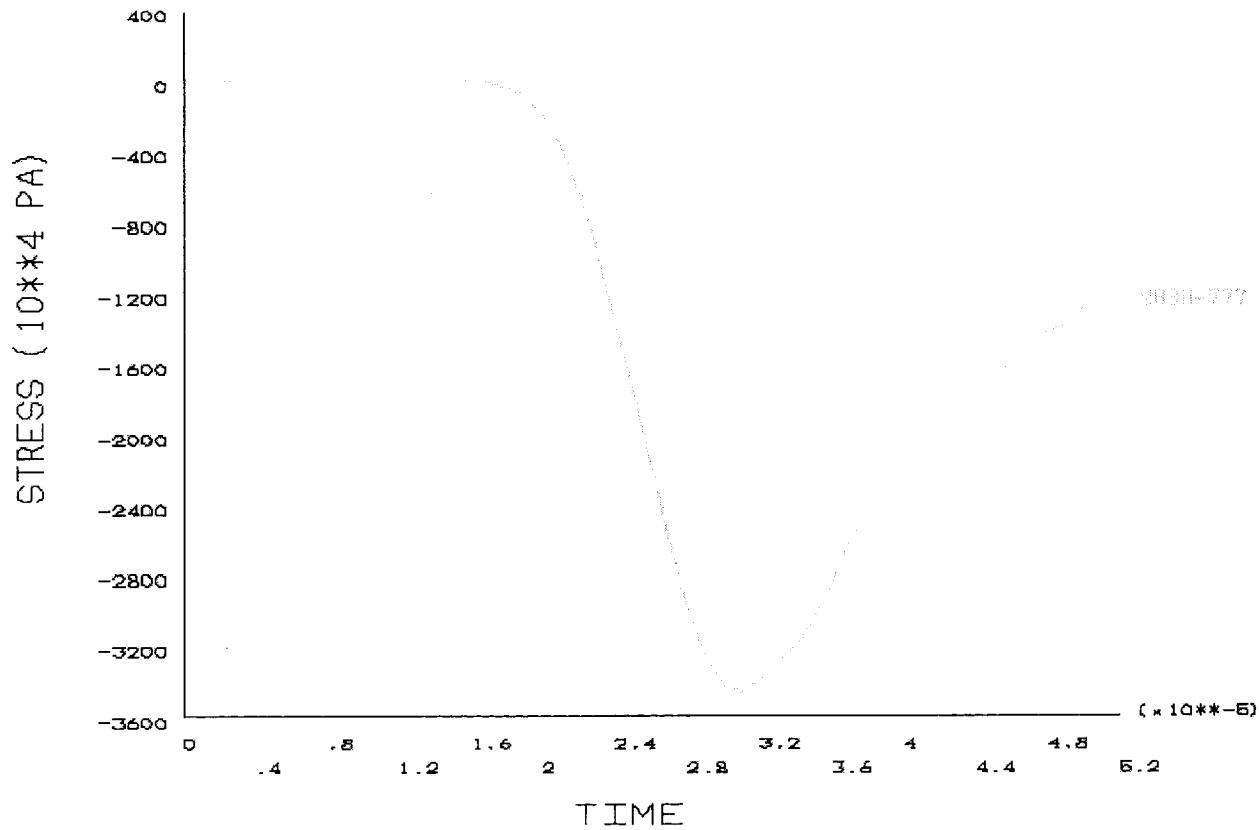


FEM results of the free-mass bounce from the drill bit. The free-mass is 2 grams and the incoming speed is 1 m/s. The rebound speed is 0.53 m/s and contact time 16 μ s.

The rebound speed is dependent to the mass of the free mass.

Free Mass - Bit Impact

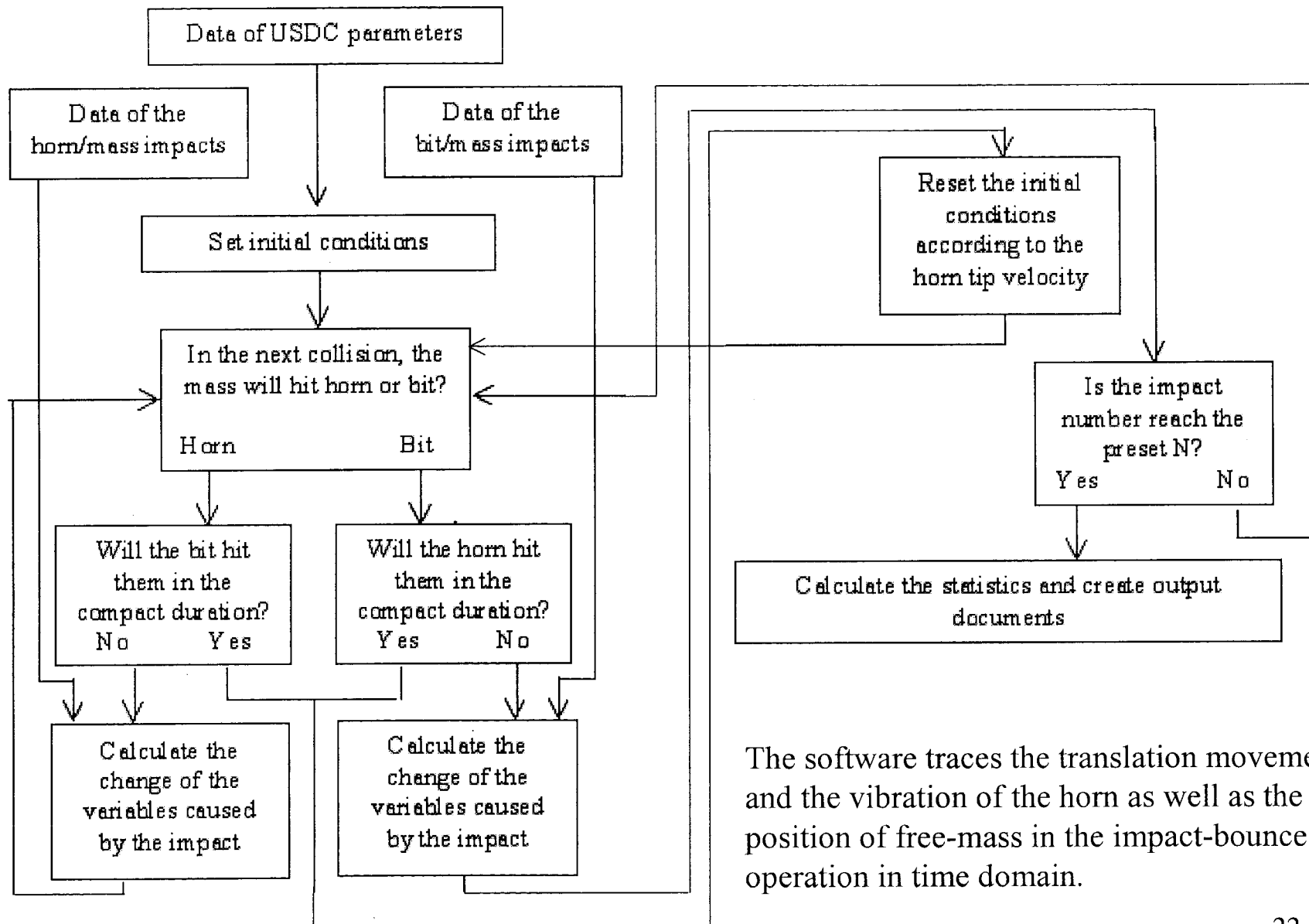
Finite Element Solution



Impact stress at the root of the bit

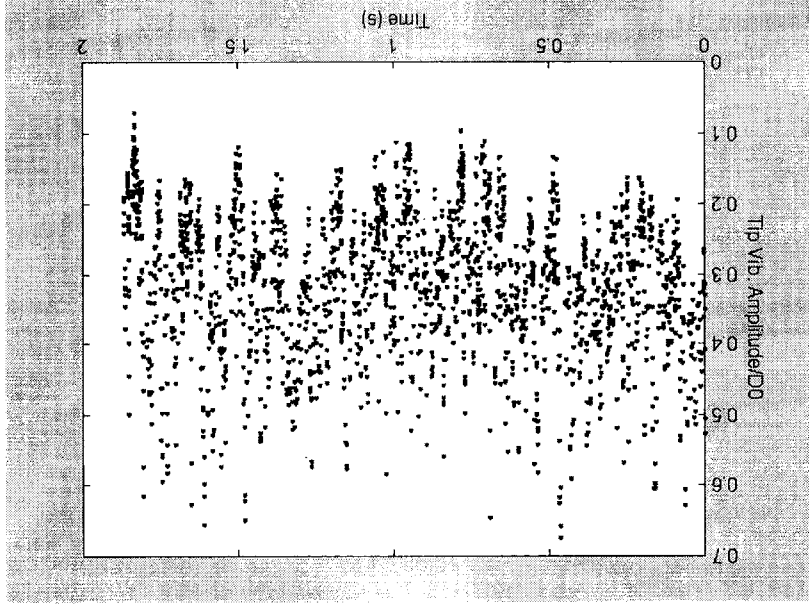
Free mass of 1 gram with 1 m/s hits drill bit D3mm x 100mm with a head of D12mm x 6mm

Simulation program

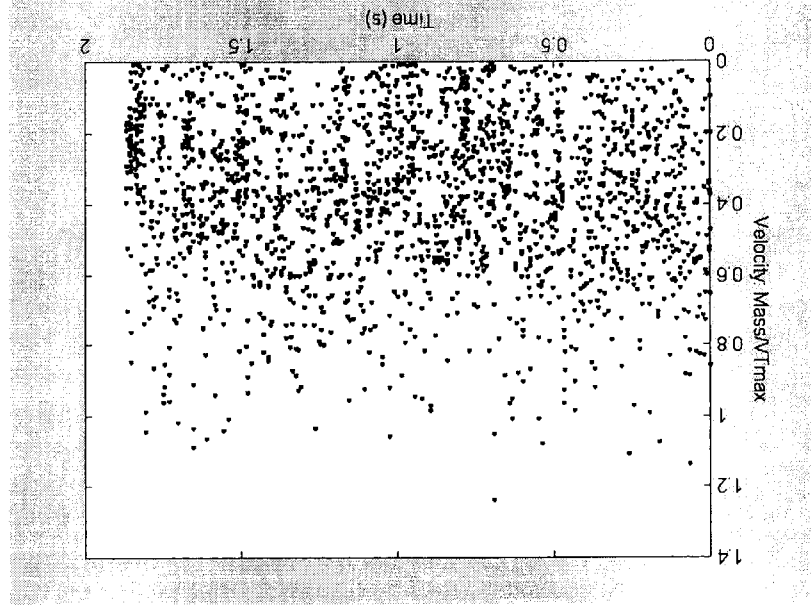


The software traces the translation movement and the vibration of the horn as well as the position of free-mass in the impact-bounce operation in time domain.

Samples of Results

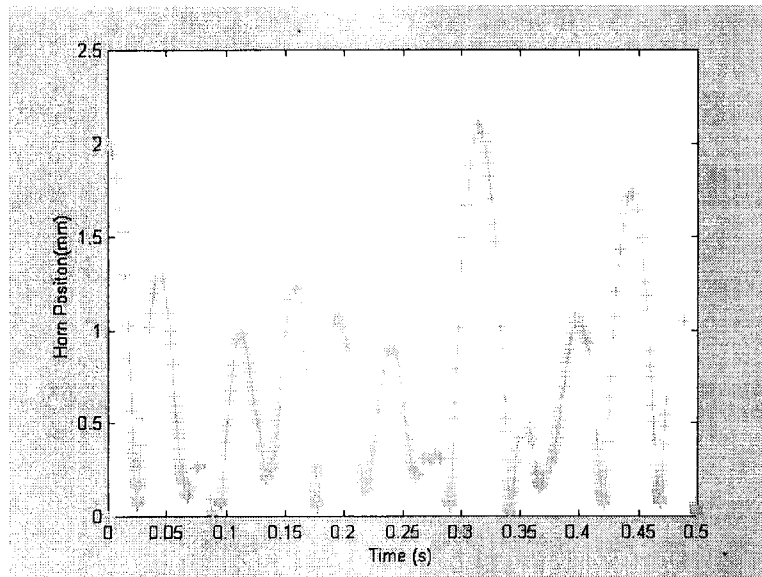


Horn vibration amplitude after impacts with free-mass normalized by the amplitude without loading



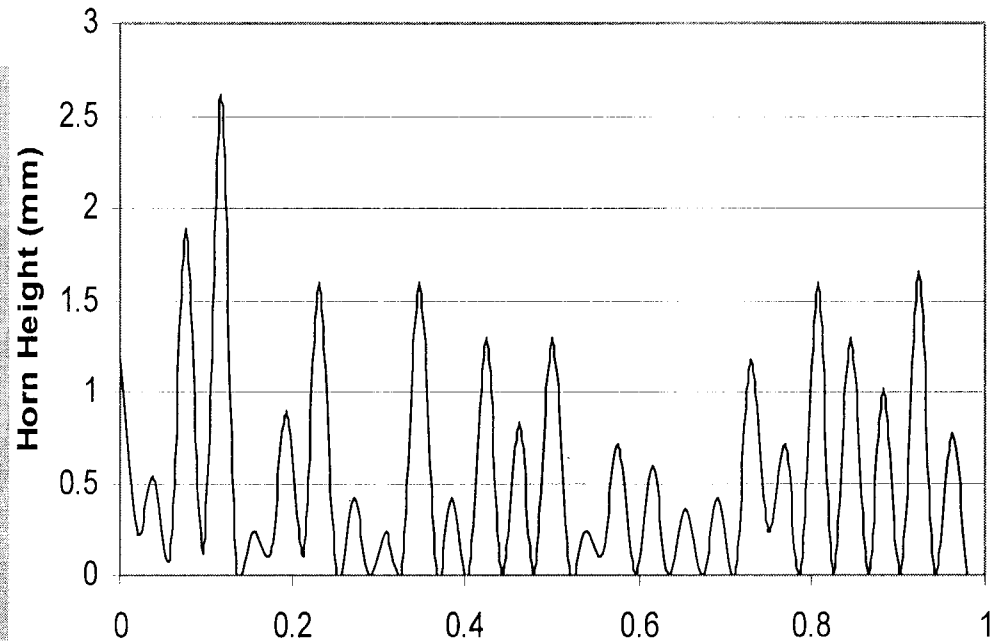
Free-mass velocity after impact with horn normalized by the horn tip vibration velocity without loading of 6.67 m/s

Motion of the Horn



Simulation Results

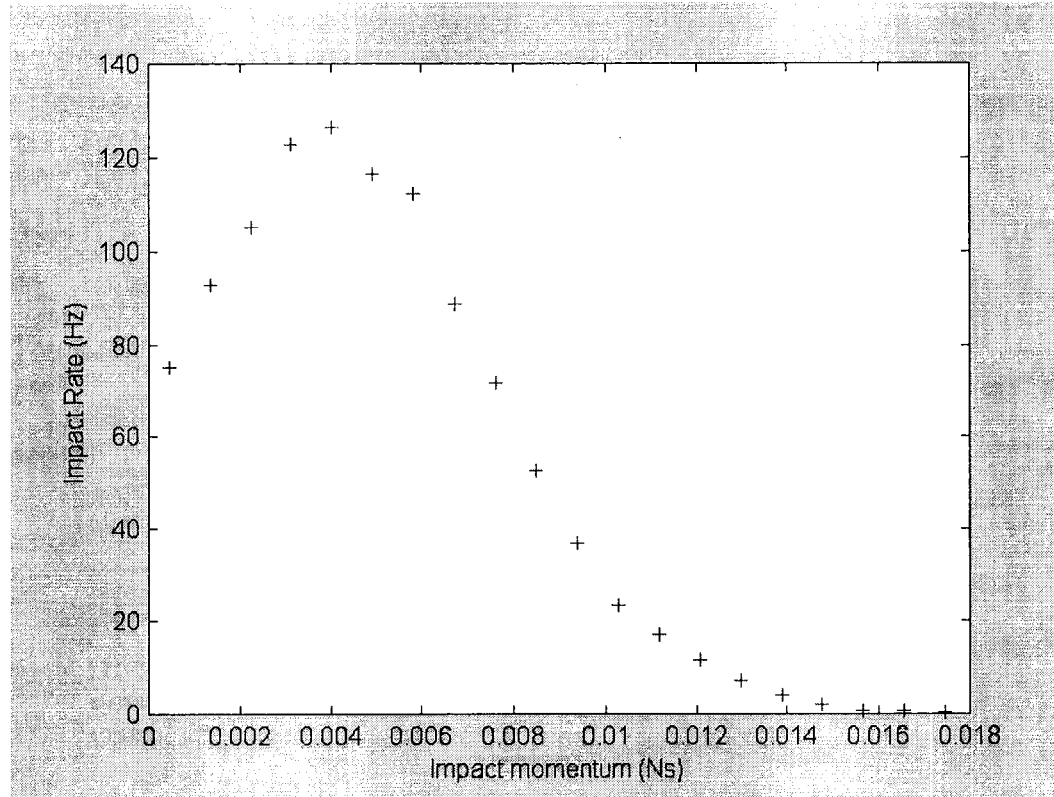
+ indicates the impacts with free mass



Experimental Data

The simulation results are confirmed by the experimental data with the random characteristics of the horn jumps and the ranges of frequency and heights of the jumps.

Statistics of Free-mass/Bit Impacts



The impact frequency versus momentum

Strain and stress in rocks

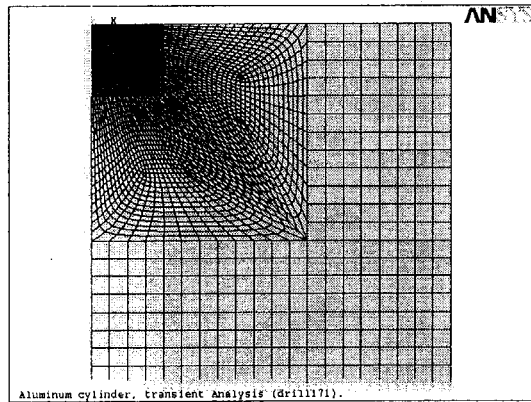


Fig. 15. The mesh used to solve the bit rock interaction.

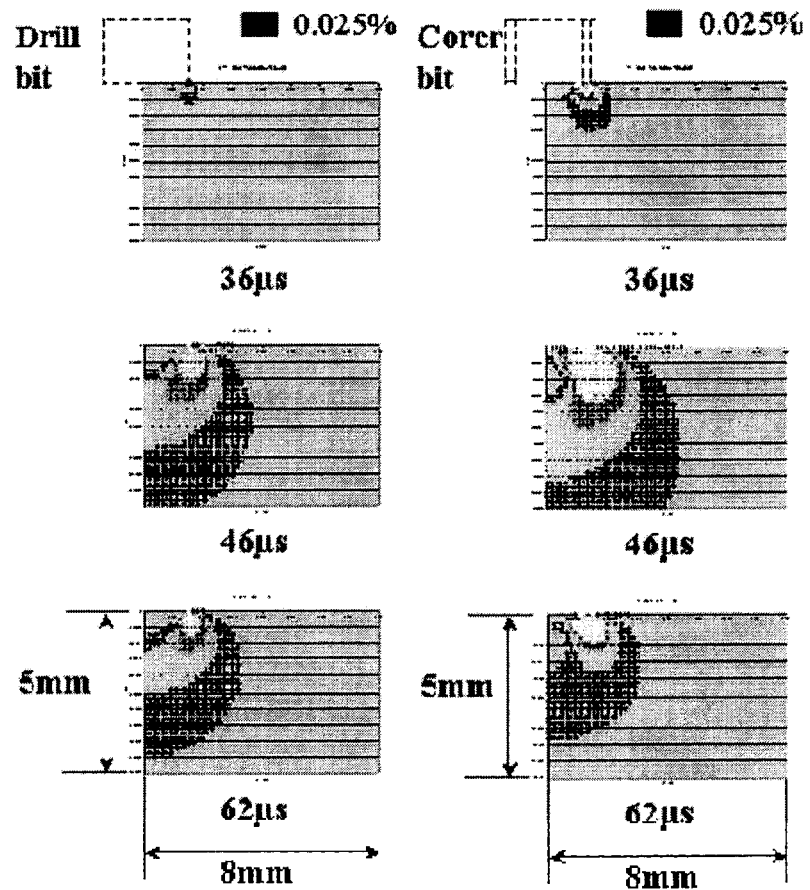


Fig. 16. The principle strain profile.

Estimation of drilling rate

Drilling rate:

$$R = P/E$$

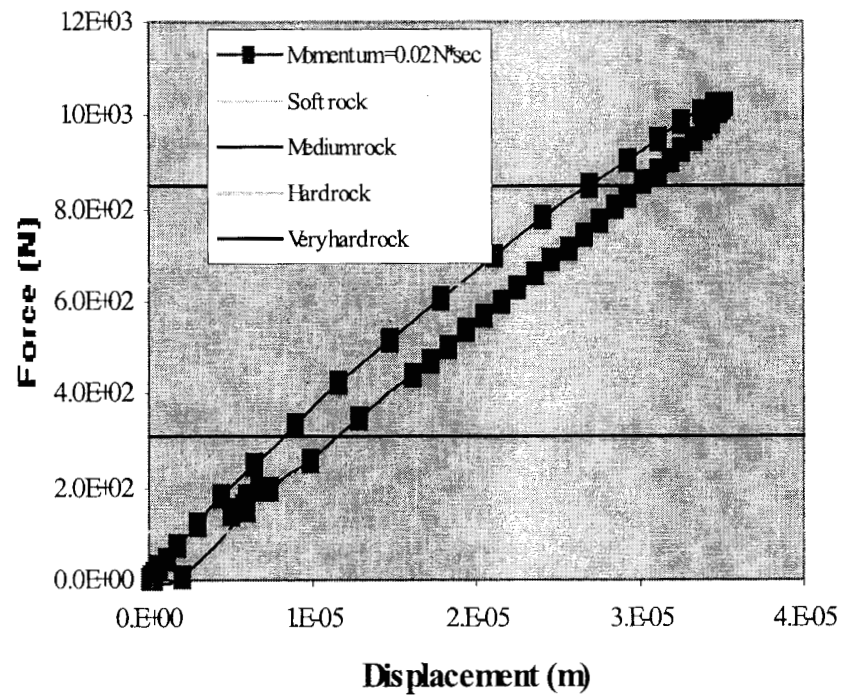
where P = power input to the rock, joules/sec

E = specific energy, joules/cm³.

Table Specific energy and compression strength of rocks*

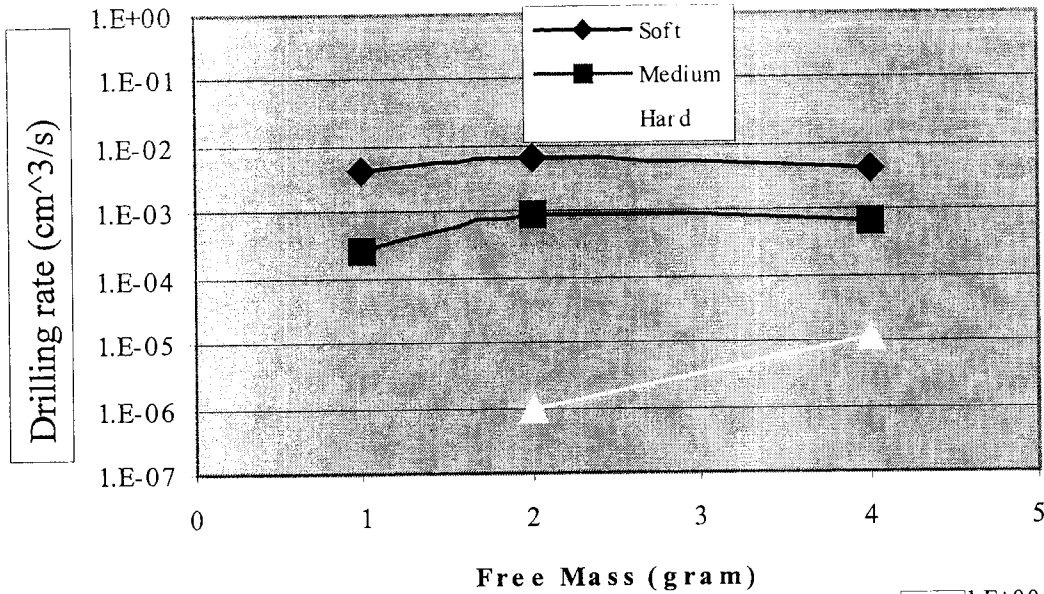
Rock type	Compression strength (MPa)	Specific energy (joules/cm ³)
Soft	< 50	30
Medium	50 - 100	50
Hard	100 - 200	260
Very hard	> 200	390

*W. Maurer, Novel Drilling Techniques, Pergamon Press, 1968



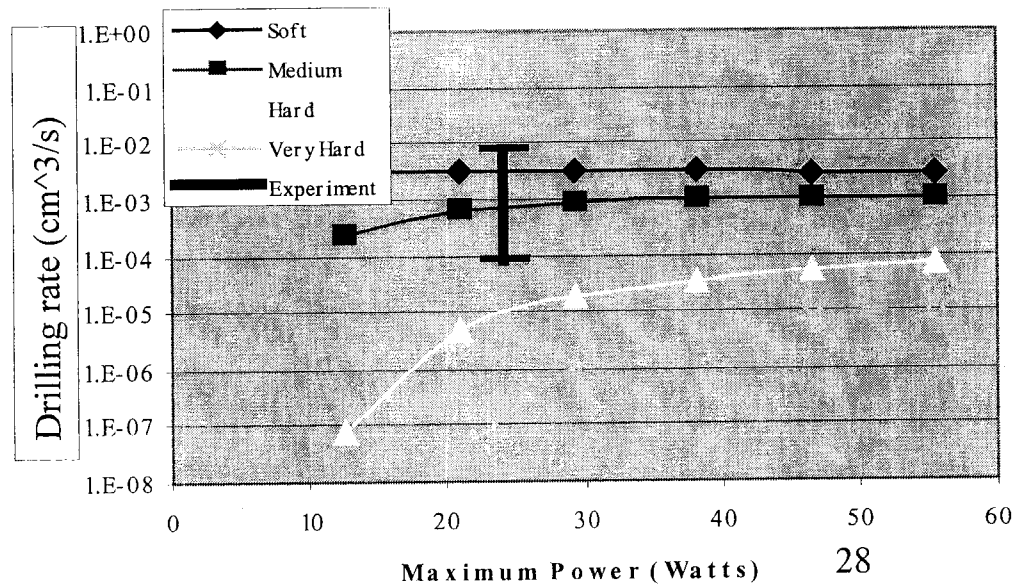
Force-displacement curve of rock surface under the drill bit.

Estimation of drilling rate

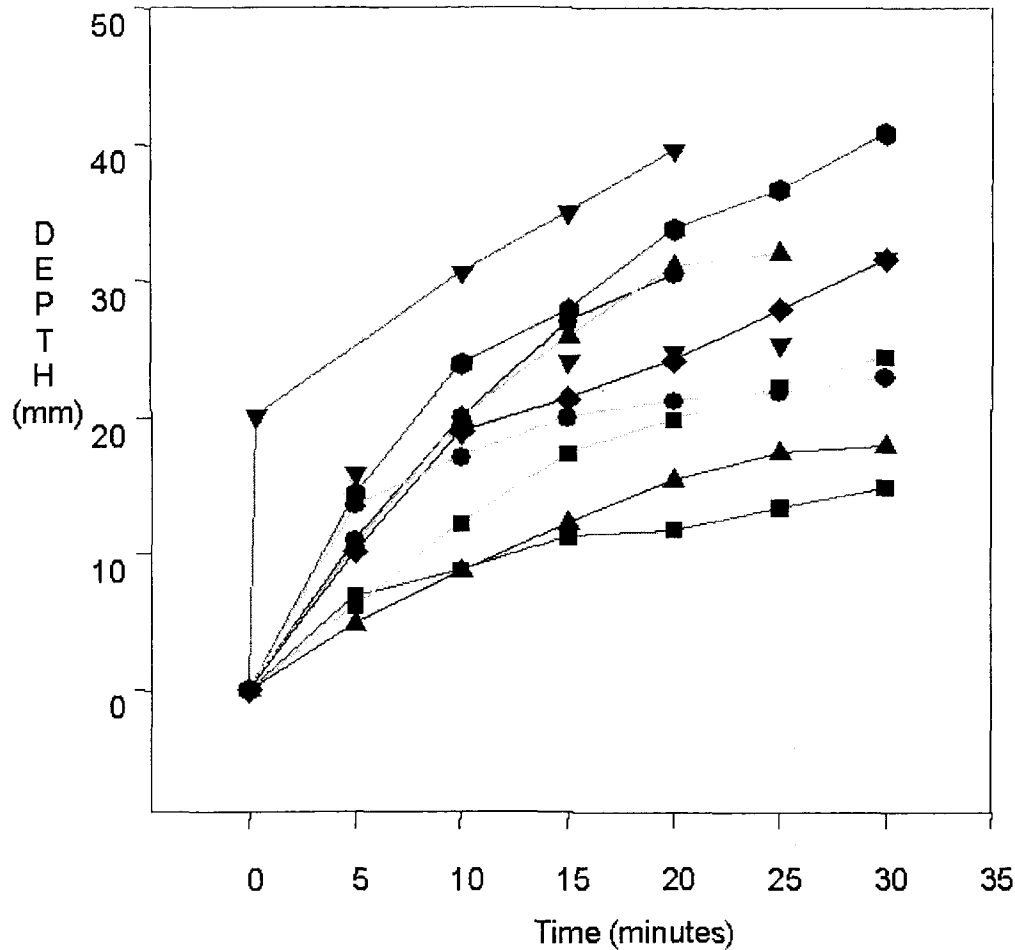


Drilling rate for different free-masses.

Drilling rate for different maximum power (the average power is maintained at 10 watts by duty cycling the power supply). The brown bar indicates the range of experimental data for a variety of rock samples.



Experimental Data of Drilling Rate



Drill bit:

D2.85 mm

Power consumption:

12 W average (24 W peak power
with 50% duty cycle)

Powder Sampling

USDC generates quality XRD powders

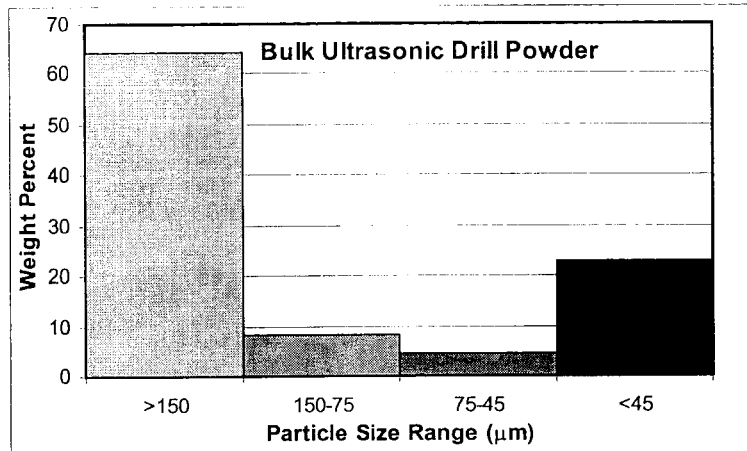


Fig.1 The size distribution of bulk powder generated by ultrasonic drill from the basal limestone of the Todilto Formation (Echo Amphitheater, New Mexico).

USDC creates large portion of fine powder that qualified for XRD analysis

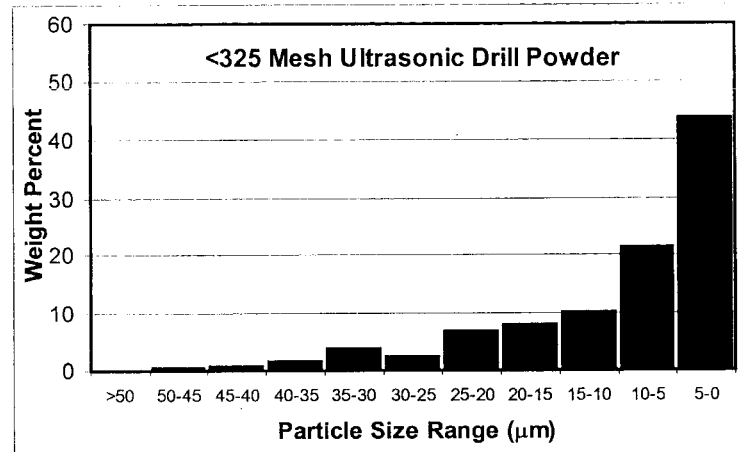


Fig. 2 The size distribution of the powder screened with 325 mesh

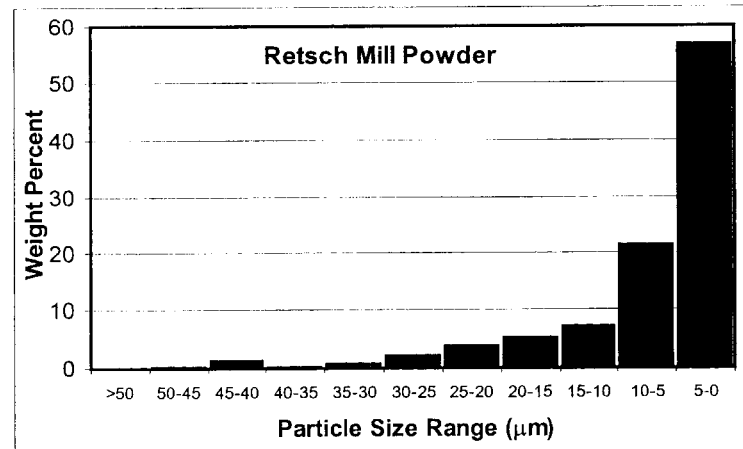
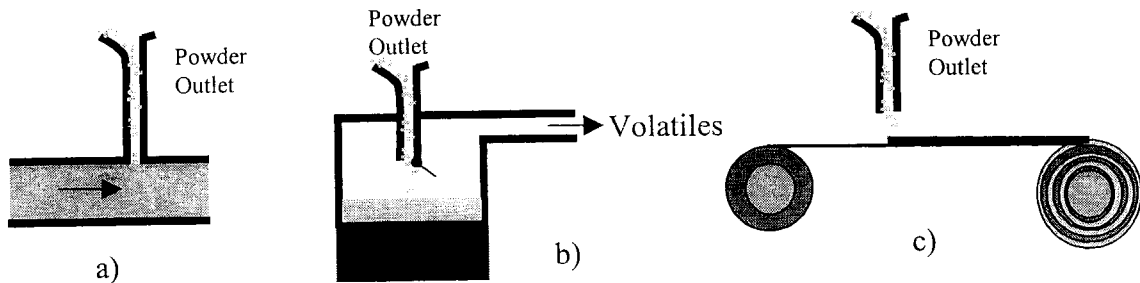
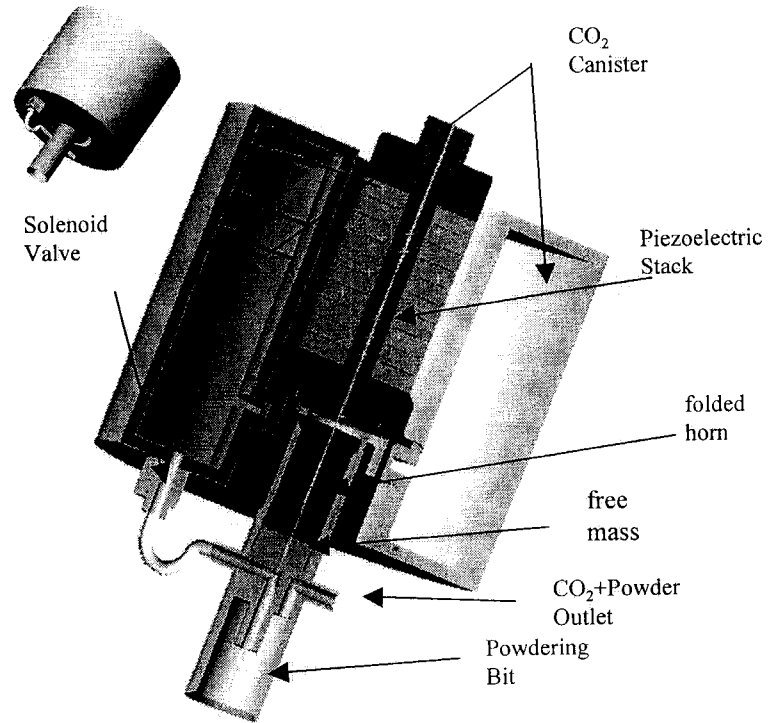
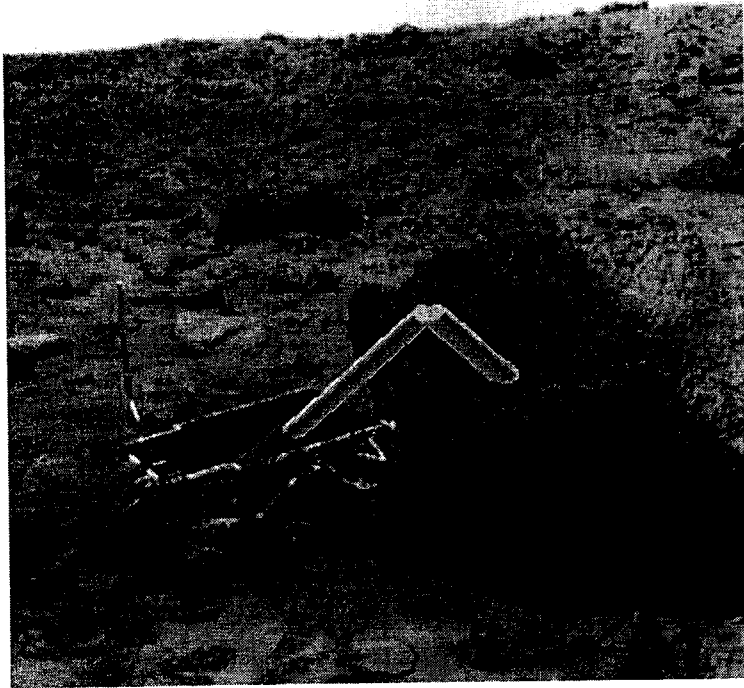
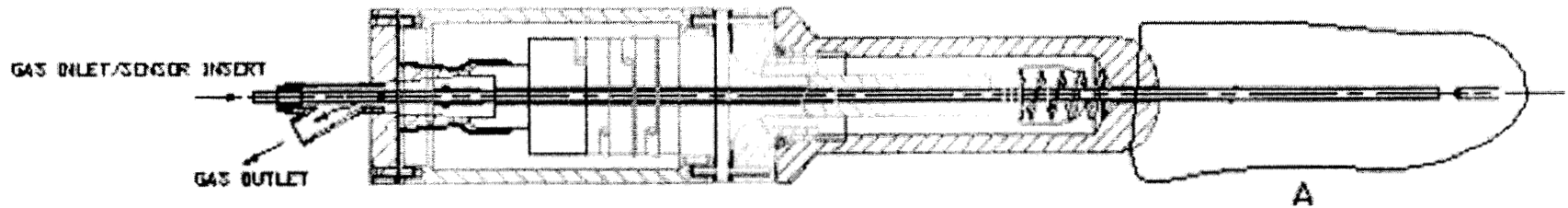


Fig. 3 The size distribution of the powder obtained from a laboratory Retsch mill

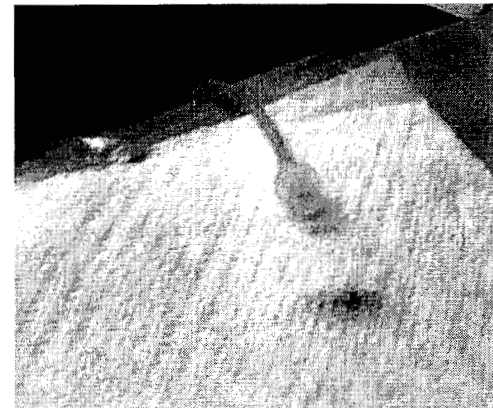
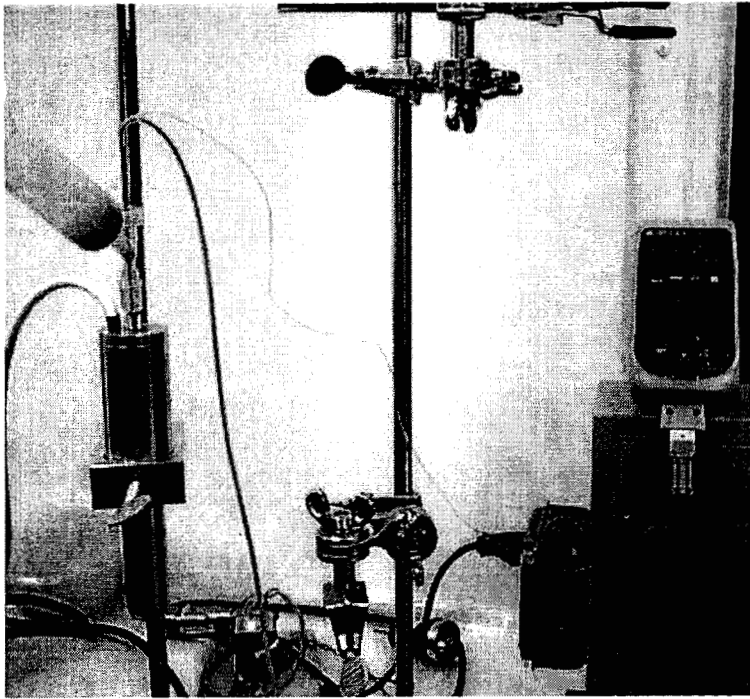
Powder Sampler



Powder sample acquisition



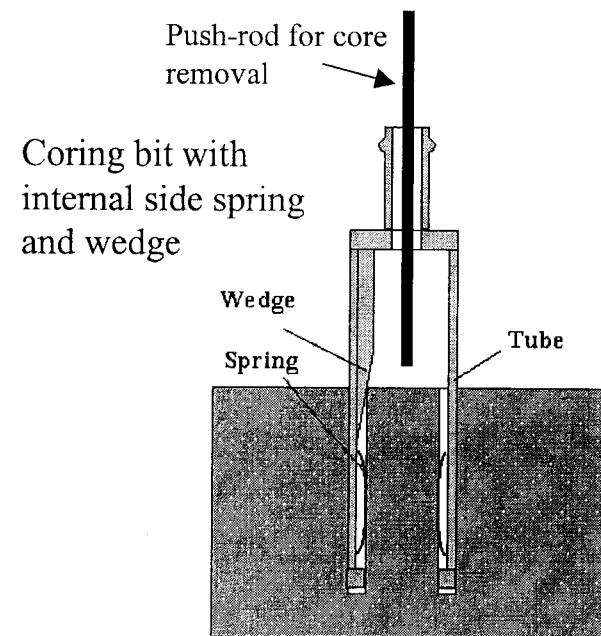
USDC with tubing and pressurized CO₂ are being integrated to allow extraction powder.



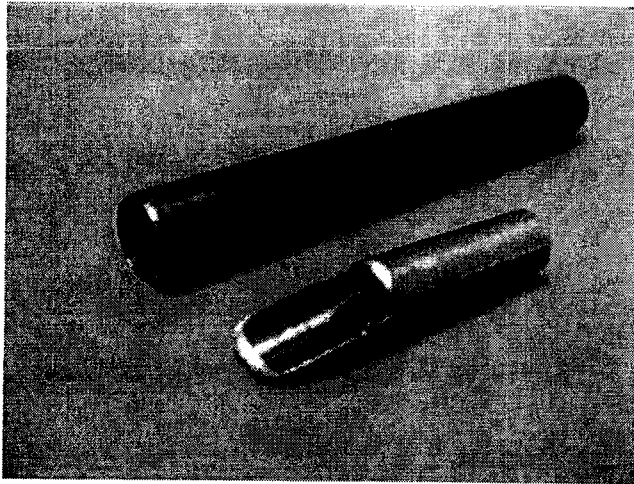
Compressed air brings the powder sample through the tube to the paper.

USDC Coring/Breaking/Holding/Extracting

- Objective
Coring/Breaking/Holding/Extracting core
- Measures
 - Using an internal wedge, the core can be fractured near the root via transverse forces
 - Thicker wall at the tip of the coring bit to prevent the core breaking during coring
 - Side springs allow detainment of the core



USDC Core Breaking/Holding Bit

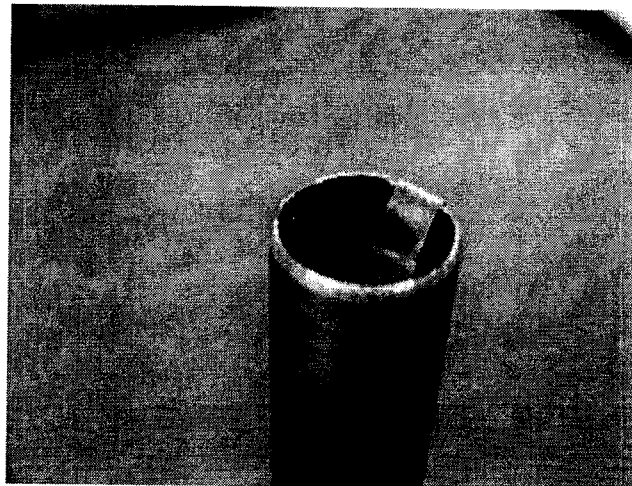


Tube and wedge



Holding spring

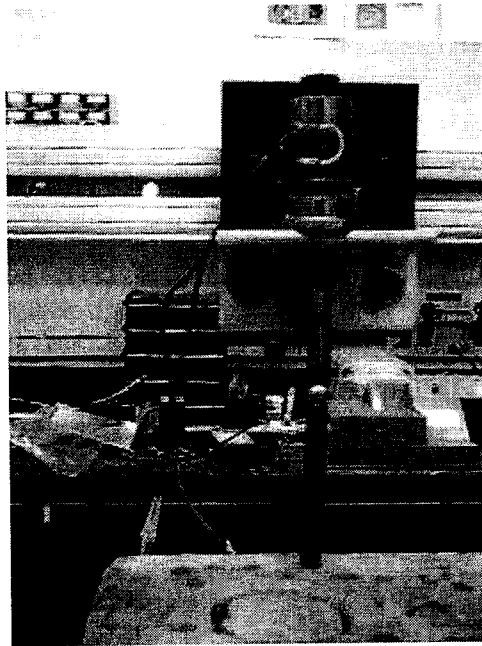
Assembled bit



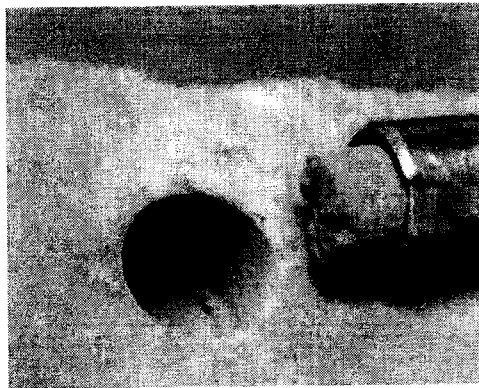
USDC Core Breaking/Holding/Extracting

Core breaking

- USDC knocking the tool down

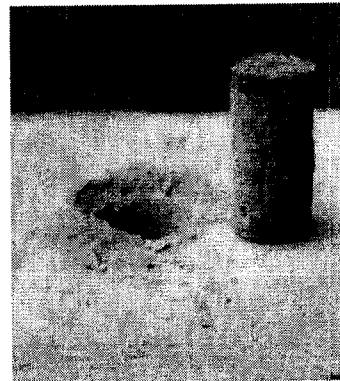


- The tool broke and holds the core.

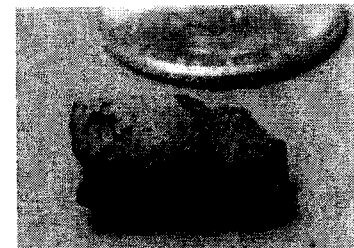


Core extraction

- Pushing by a bar
The sample may be hold by the wedge tightly and results in damage of the sample.



D6 x 12 mm core



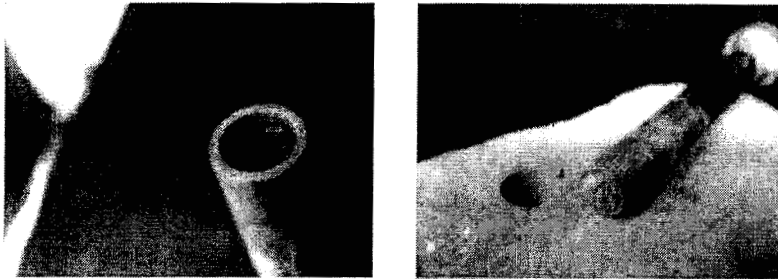
Damaged sample

USDC Coring/Breaking/Holding/Extracting

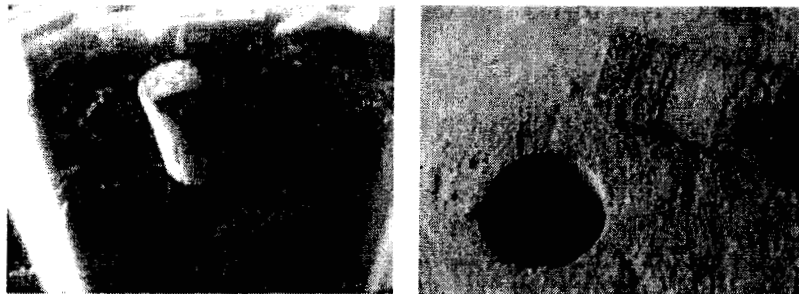
All in one bit using an internal wedge and an internal side spring

- This mechanism was tested on bricks
- Two D6 x 15 mm cores were created out from two attempts
- Side springs allow detainment of the core
- An alternative method for extraction of the core from the coring bit, by using the USDC horn successfully “kicked” the core out.

Detainment spring and a grabbed core

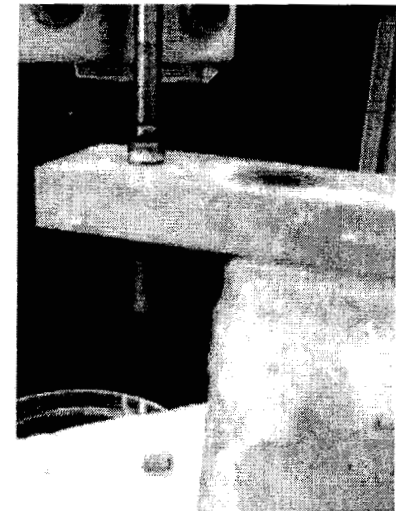


Two created cores (out of two attempts)



Core extraction

- “kicking” the core out using the USDC.

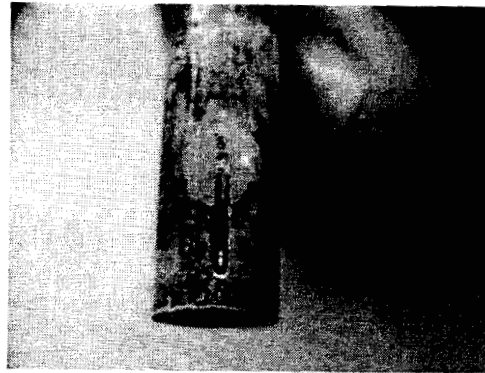


USDC Coring/Breaking/Holding/Extracting

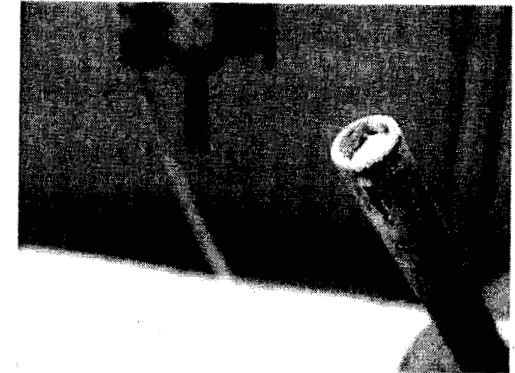
All in one bit for rock may be fractured

- Fracture the core continuously in coring process by control of coring parameters such as core diameter, bit wall thickness, off-axis vibration
- Using a side spring to hold broken core pieces
- The formation of pieces and their continued vibration lead to their rounding.

- USDC bit: With an embedded spring near the tip
- Sample: limestone block.
- Drilled depth: D6 x 20-mm

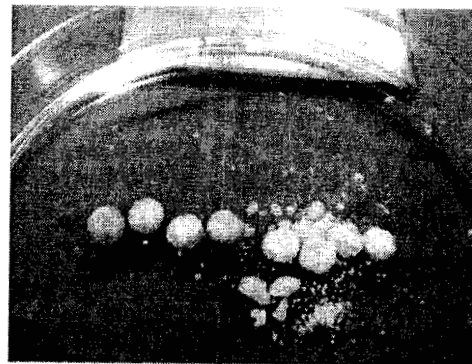
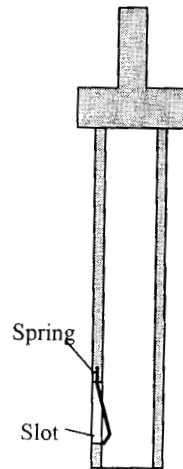


Coring bit with a side spring near the tip

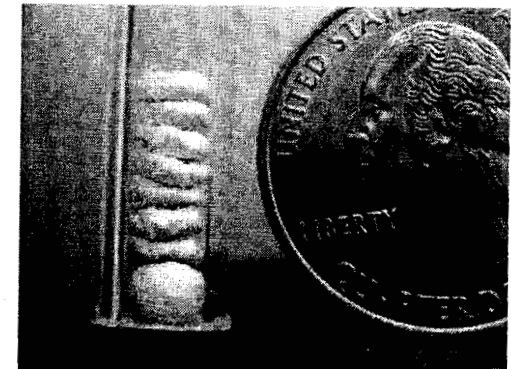


Core retained inside the bit

Coring bit with the side spring for bit detainment



Extracted samples

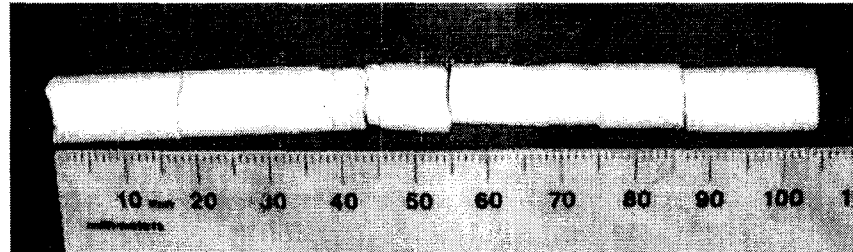


Stack of 17-mm high 8 core pieces

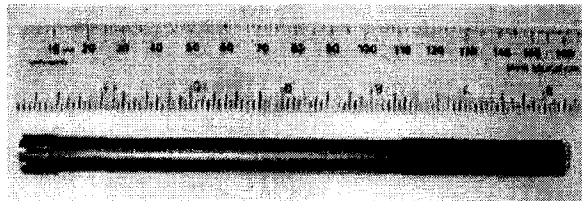
Coring via the USDC

By controlling the power and wall thickness (0.25 mm) of the coring bit, a D9x100-mm total long limestone core was obtained with reasonable piece-length:

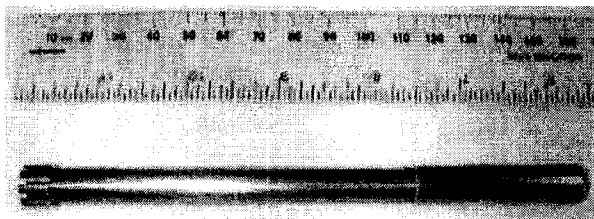
- 94.6 minutes with the drilled depth of 110-mm.
- The average power to actuator was 9.6 W (averaged working power 16 W).
- The total energy to the actuator was 15 W·hour.



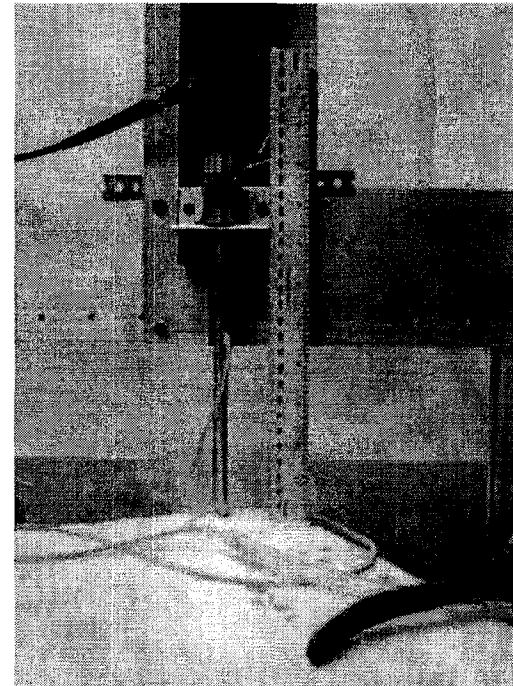
Bits made of high quality alloys



A bit made of Ferro-Tic



A bit made of Vascomax



A view of the USDC and the coring bit used to sample the above core, where a dust removal tubing was used.

Self-Rotating Coring Bit

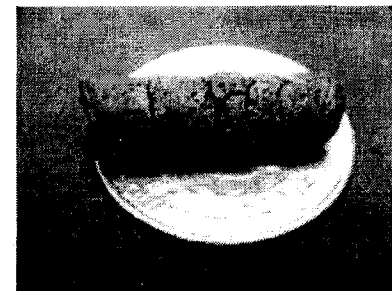
Auto rotating in coring process

- Advantages of rotating bits
 - Preventing the bits from getting occasionally stuck in the holes.
 - Help to make more straight holes.
 - Improve drilling efficiency of the bits with teeth.
- Mechanism
 - Two helical slots was made on the side wall.
 - Under the downward impact of the free mass, the helical structure creates a rotating component for upper part of the bit.
 - The inertia of the upper part brings the lower part of the bit rotating after the impact.
- Test
 - On a basalt rock
 - Rotating at tens rpm.

Self-rotating coring bit with helical slots and free mass on the top. The arrow shows the rotating direction.



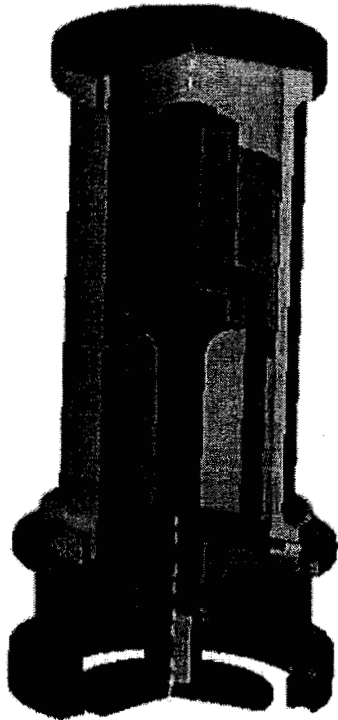
Sampled core of D7 x 23 mm from a basalt rock. The core was broken to 6 pieces which are able to be put together.



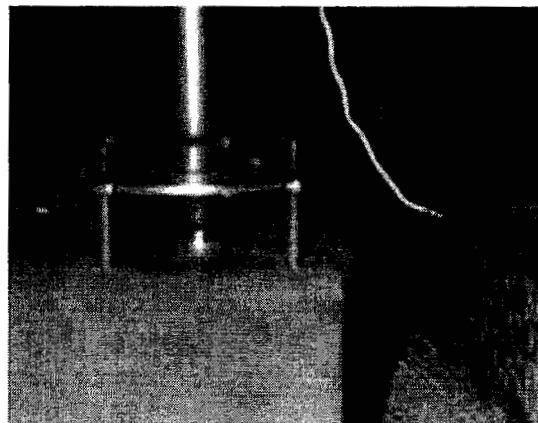
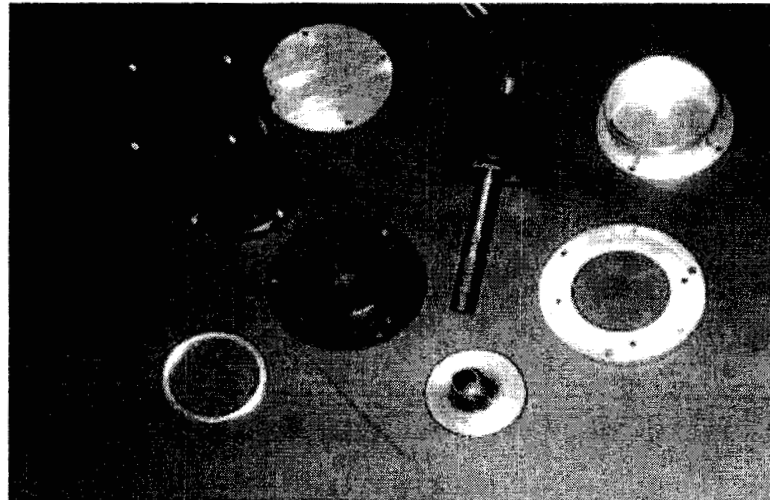
URAT: Ultrasonic Rock Abrasion Tool



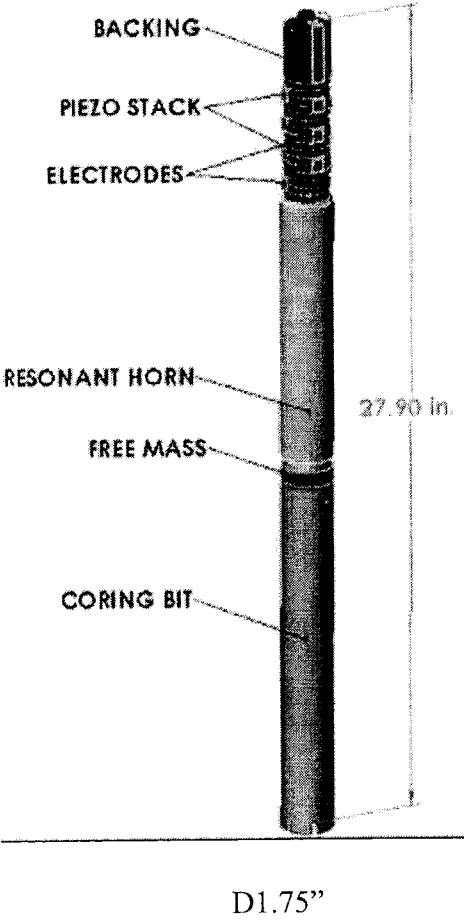
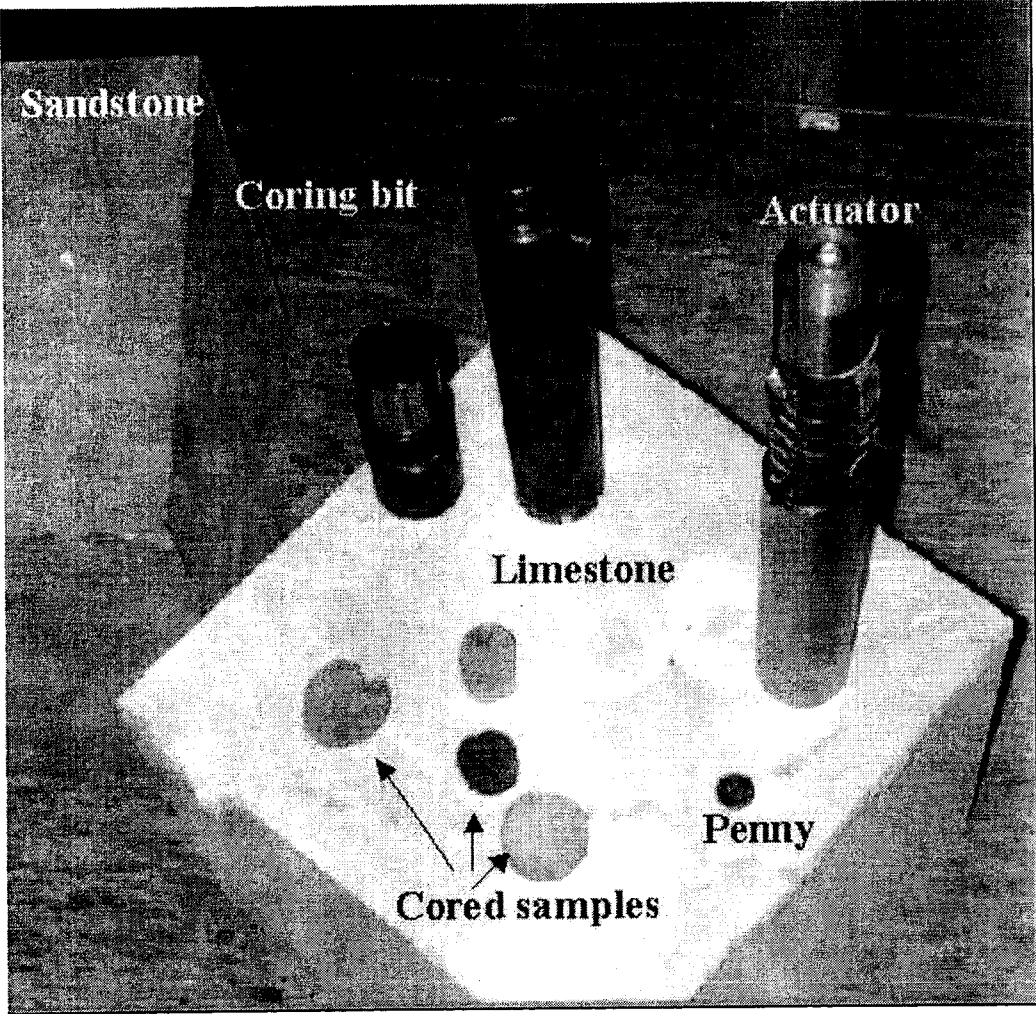
URAT Schematic and Disassembled



Abrading
brick



Ultrasonic Gopher



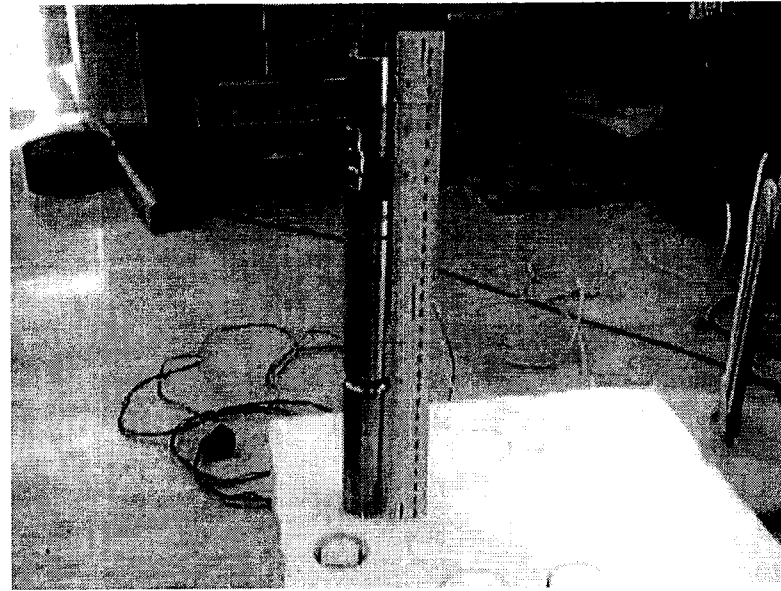
Ultrasonic Gopher

Another design



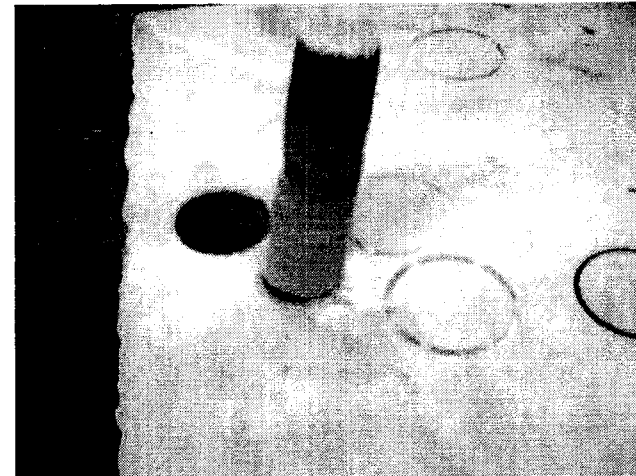
- **The Gopher**

Size: D1.125" x 12"
15 kHz



- **Core and the hole on limestone**

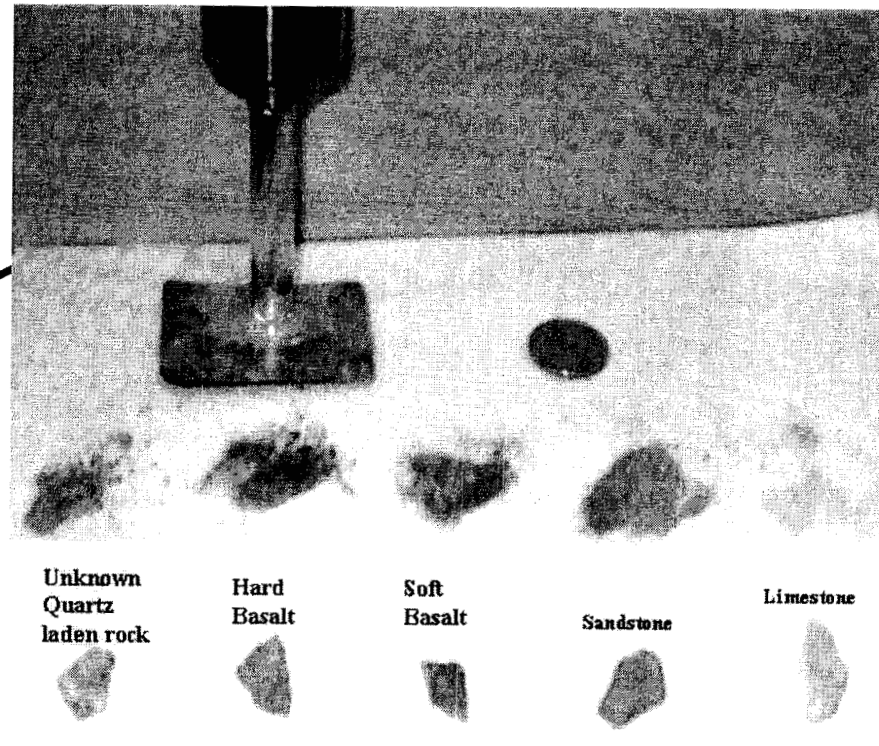
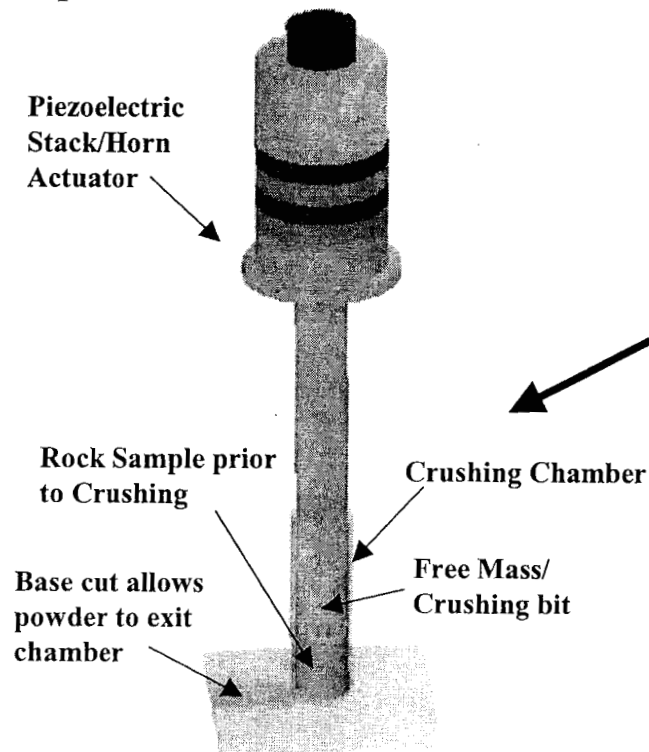
Core D1" x 4"



Powdered Cuttings

USDC crusher

- The USDC is used as a rock crushing, milling, and powdering device.
- Its actuator harmonic motion creates a series of low frequency impacts that grind the sample into powder within a short time period.
- A crushing chamber confines the free-mass to movement in one direction only leading to a very efficient milling.
- The grinding effect can be enhanced by making a free-mass with teeth on its interface with the sample.

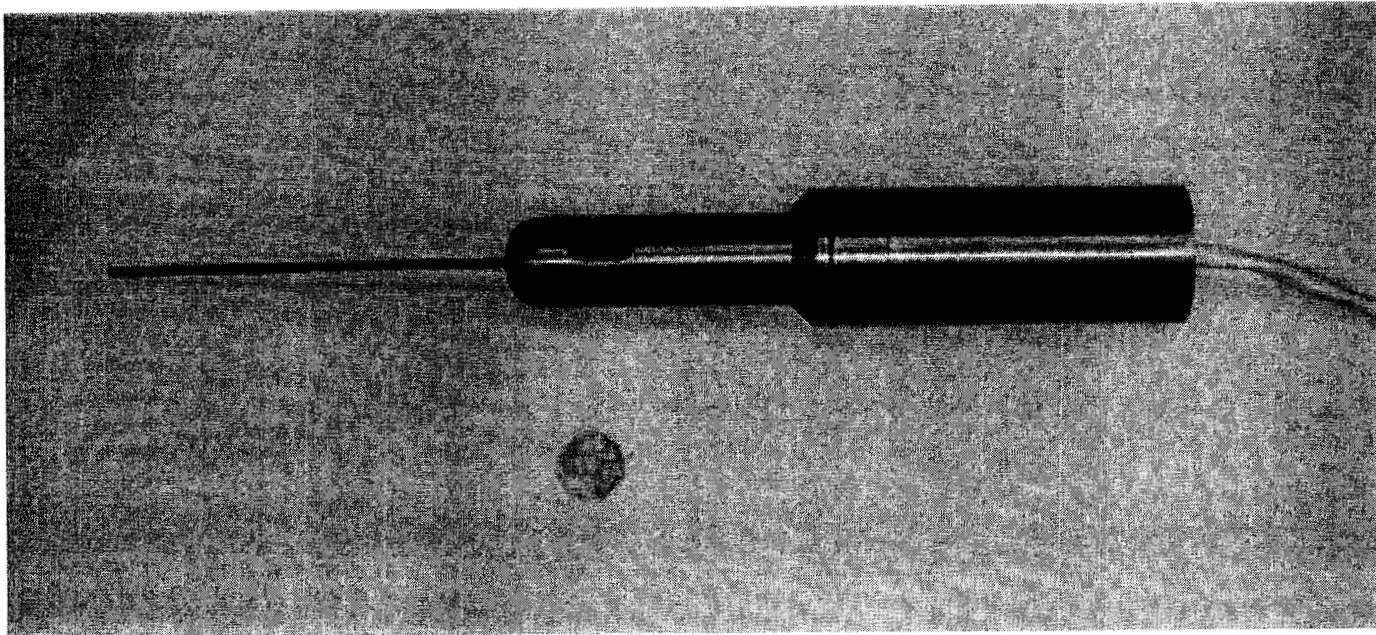


High temperature USDC for Venus



HT-USDC

A USDC that can operate at 450°C would be applicable for the exploration of Venus.



EAP MATERIALS and EAP MIRROR

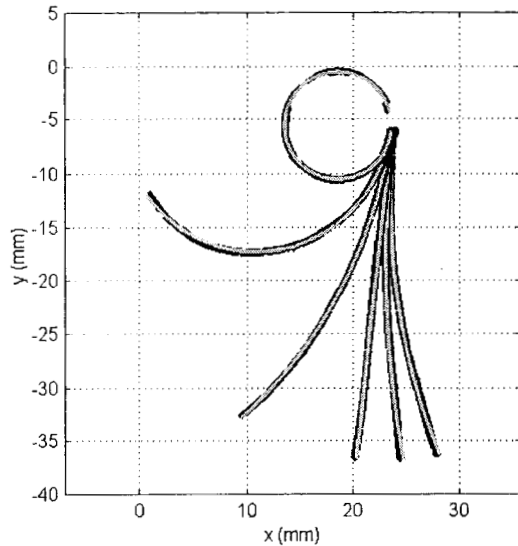
- Ionic EAP's
 - Contain electrolyte in a polymer frame.
 - Large bending deformation at low voltage excitation.
 - The component and properties of the electrolyte have to be maintained well to keep the performance stable.
- Electric field EAP
 - Piezoelectric, electrostrictive, ferroelectric or dielectric polymers etc.
 - Thickness and length deformation under voltage ($10 \sim 100\text{V}/\mu\text{m}$) excitation. Bending with unimorph or bimorph structures.
 - Solid phase, relatively stable.

Numerical modeling of single-layer electroactive polymer mirrors for space applications, Bao X, et al, Paper 5051-45, Proceedings of the SPIE Smart Structures Conference, San Diego, CA., Mar 2-6. 2003

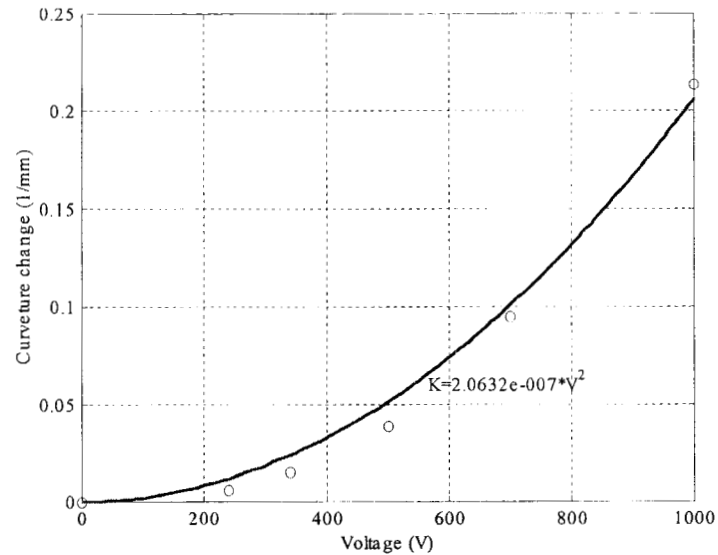
DEFORMING CAPABILITY OF EAP

Electron irradiated P(VDF-TrFE) copolymer

Samples provided by Dr. Qiming Zhang, Pennsylvania State University



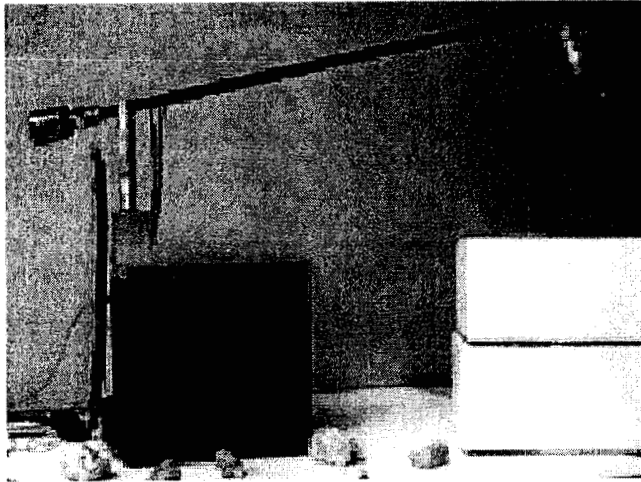
Circle fitting for unimorph S1 under 0, 240, 340, 500, 700 and 1000 V



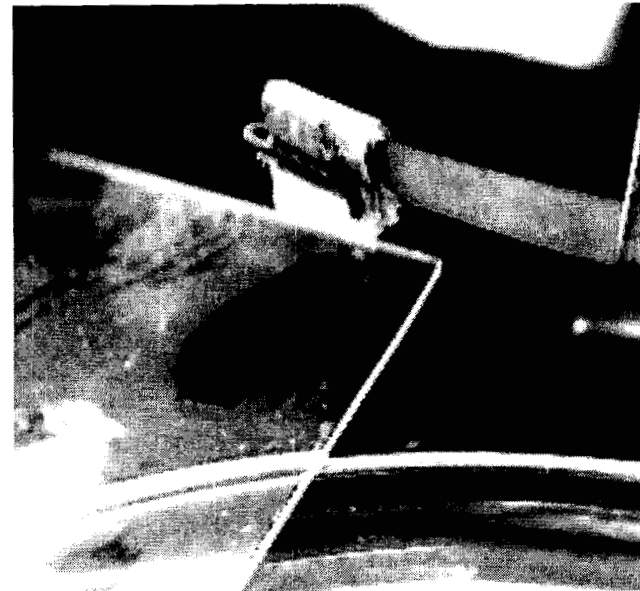
Curvature change of the sample S1 by applied voltage

Sample	T_{total}	W_{total}	$K_{@1KV}$	$F_{@1KV}$	R	E_{eq}	$\epsilon_{@100V/\mu m}$
	μm	mm	m^{-1}	$10^{-3}gf$	Nm^2	10^9Pa	%
S1	63	3.9	215	196	6.56E-08	0.808	3.2

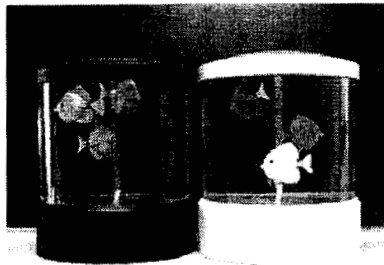
EXAMPLES OF APPLICATIONS



4-finger EAP gripper that is lifted/dropped by an EAP actuator



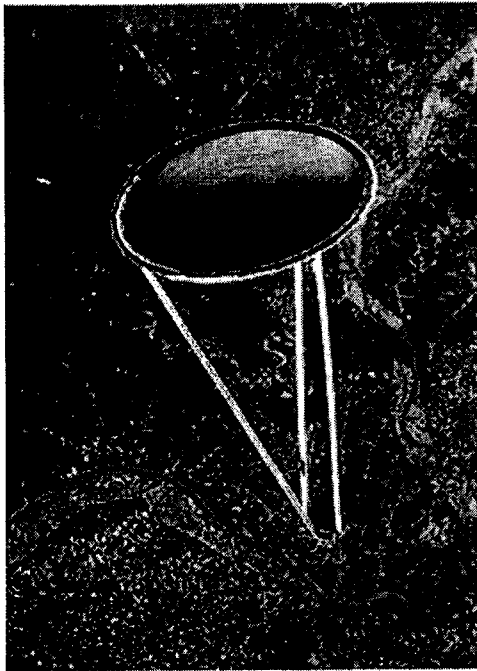
A IPMC brush cleaned bio-contaminated glass (for sensor in water reclamation system)



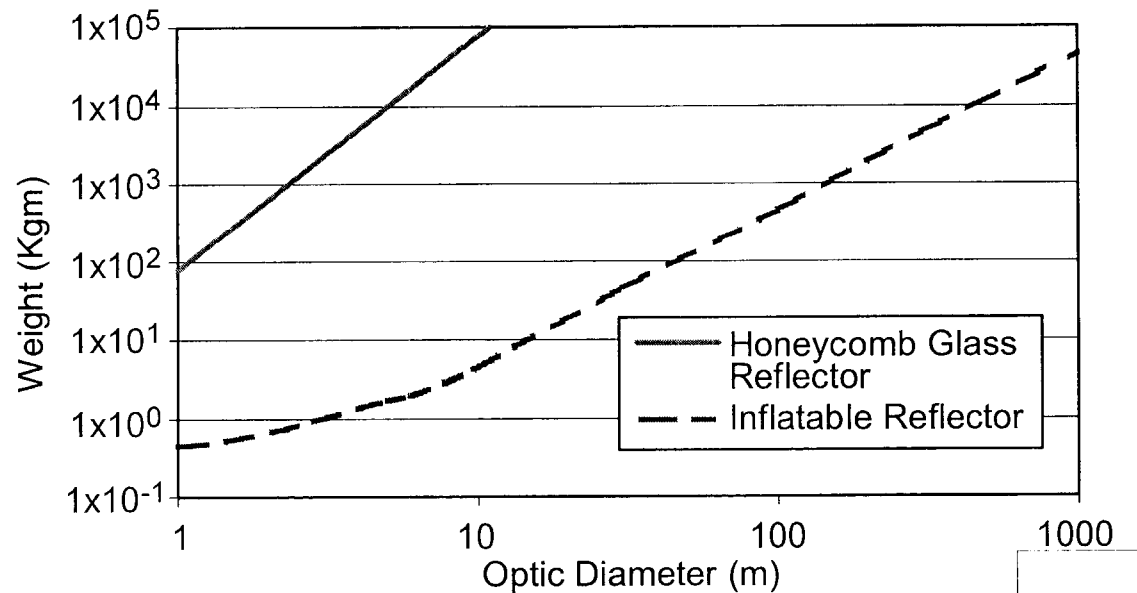
Commercial robot fish, EAMEX; Japan

EAP MIRROR - INTRODUCTION

- Thin-film mirrors for large apertures, lightweight optical systems and microwave antennas operating in micro-gravity space are attractive.



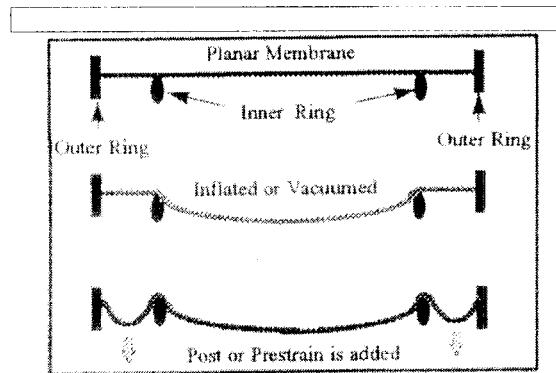
132-pound 50-foot-diameter inflatable antenna, STS-77.



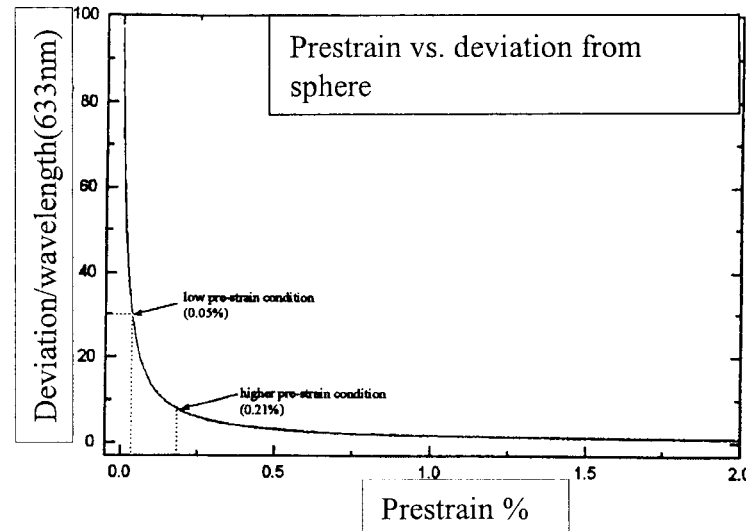
Glass and inflatable optic mass as a function of diameter.

CONTROLLABLE THIN-FILM MIRRORS

- The surface shape of these deployable thin film structures requires control to a precision range that depends on the specific applications.



Inflatable mirror with doubly curved surface, D=28cm



D. Marker, et al, "Optical evaluation of membrane mirrors with curvature," SPIE V3430, 202-208(1998)

- Electroactive polymers (EAP) are one of potential candidates of the actuation materials
 - EAP film can be both the structural and the actuation material of the mirrors.
 - Capability to realize distributed actuation to the whole mirror surface .

Concept of distributed shape control of piezoelectric bimorph mirror

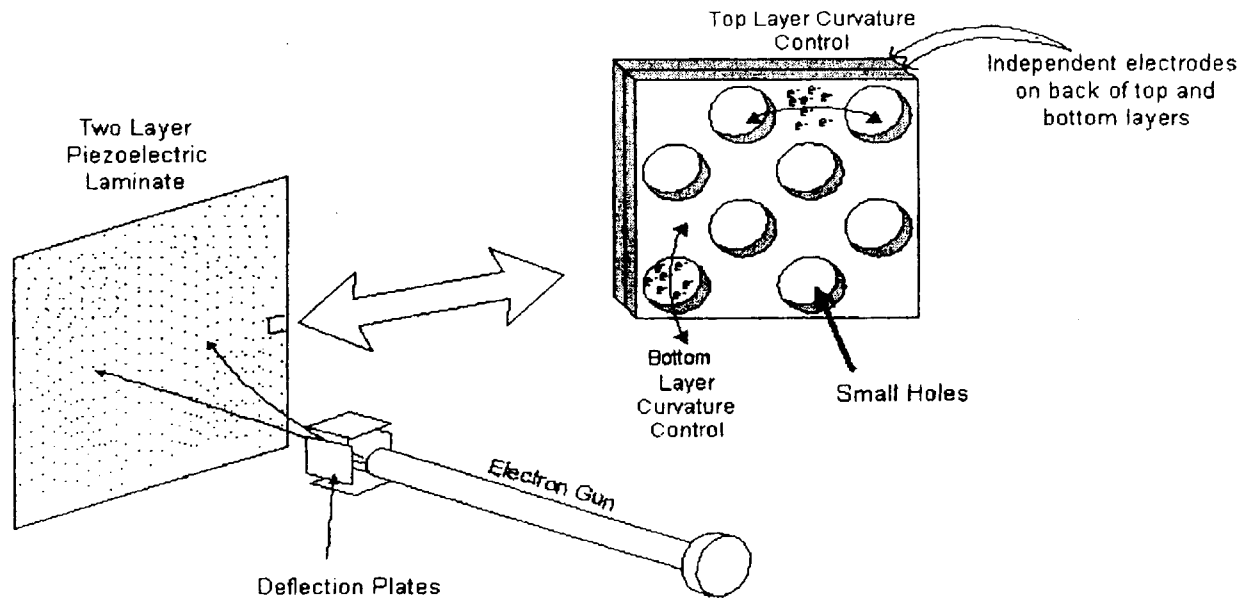
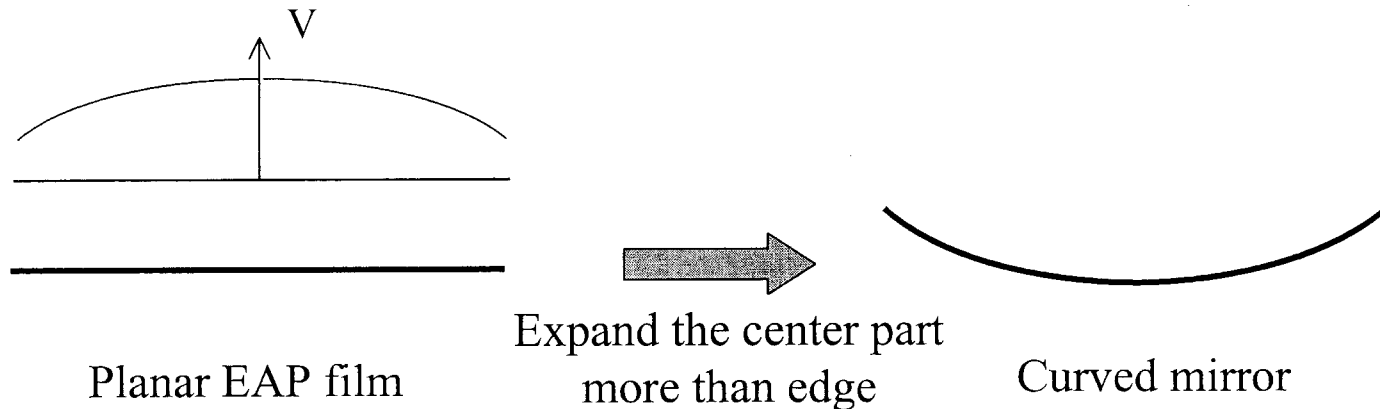


Figure 12. Conceptual design of a bimorph mirror designed for independent layer control using a single electron gun source.

- J. W. Martin, et al, “Distributed sensing and shape control of piezoelectric bimorph mirrors,” *J. Intell. Mater. Sys. Struc.* v 11, p 744-757, 2000. (Sandia National Lab and University of Kentucky)

SINGLE-LAYER EAP THIN-FILM MIRROR

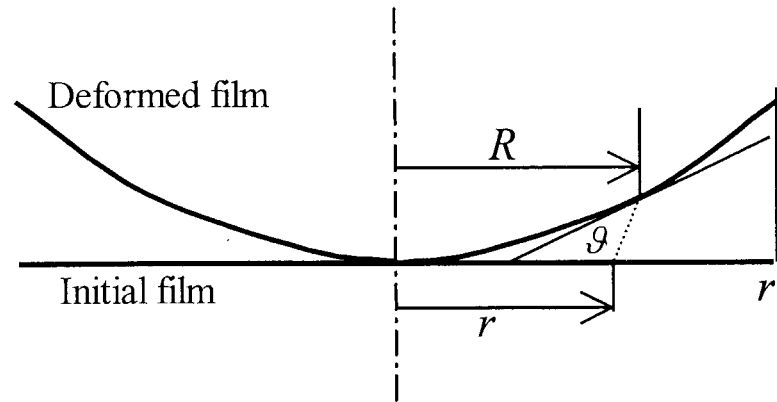
- We propose a controllable mirror of single-layer EAP film.
- Using isotropic, electric field EAP.
 - Simpler configuration.
 - Better controllability.



MODELING

- Solve the inverse problem:
 - find required voltage/deformation for desired mirror shape.
- Assumption:
 - the film is thin enough, so the bending stiffness can be neglected.
- Set the in-plan stress to zero in deformed mirror.
 - Any negative in-plan stress (compression) that will result in further buckling of the thin film.
- The desired surface is parabolic with the same diameter as the original planer film.

FORMULATION



Parabolic curve

$$z = ar^2$$

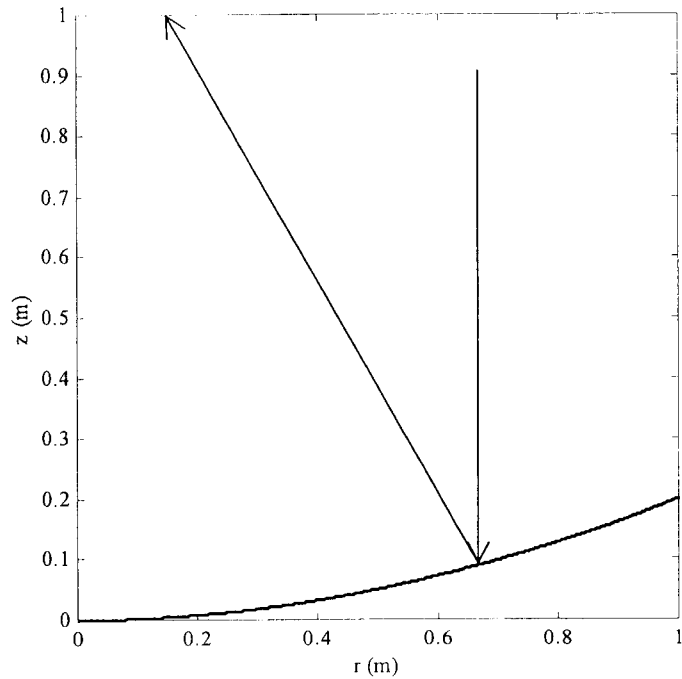
Solution

$$\sqrt{1 + 4a^2 R^2} - a \tanh\left(\frac{1}{\sqrt{1 + 4a^2 R^2}}\right) = \ln(r) + c$$

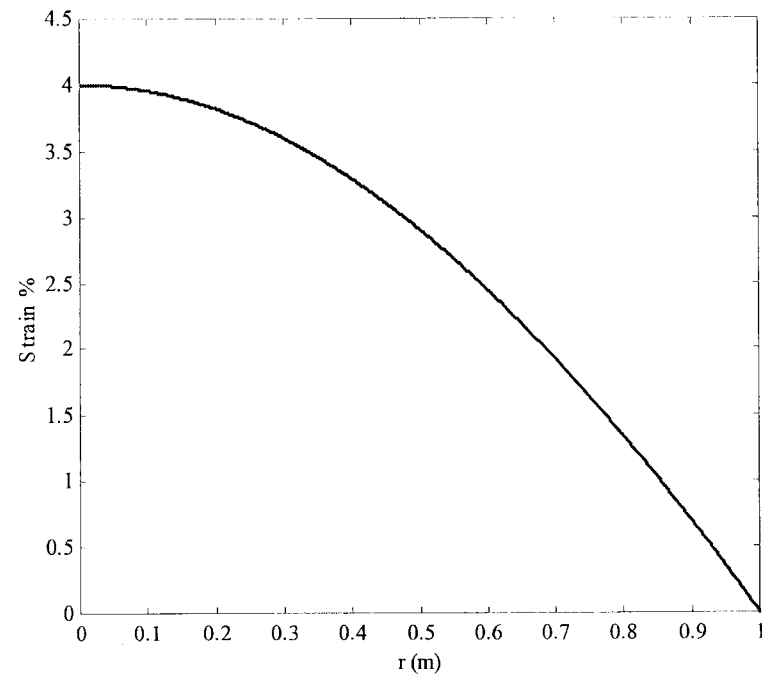
constant

$$c = \sqrt{1 + 4a^2 r_1^2} - a \tanh\left(\frac{1}{\sqrt{1 + 4a^2 r_1^2}}\right) - \ln(r_1)$$

COMPUTED RESULTS



The target paraboloid is $z = 0.2r^2$
2 m in diameter
focus distance 1.25 m,
 $f/D=0.625$.

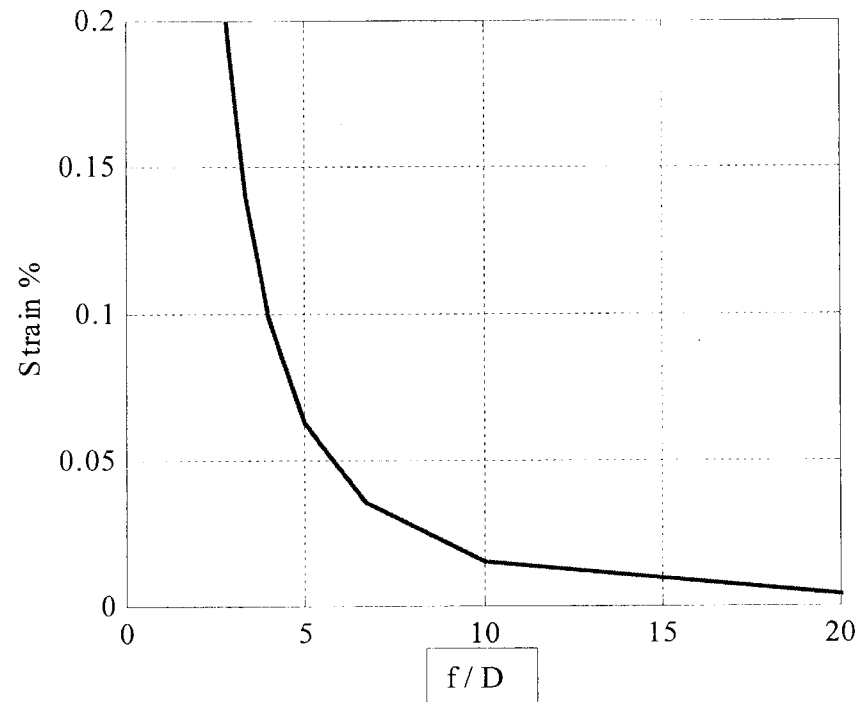
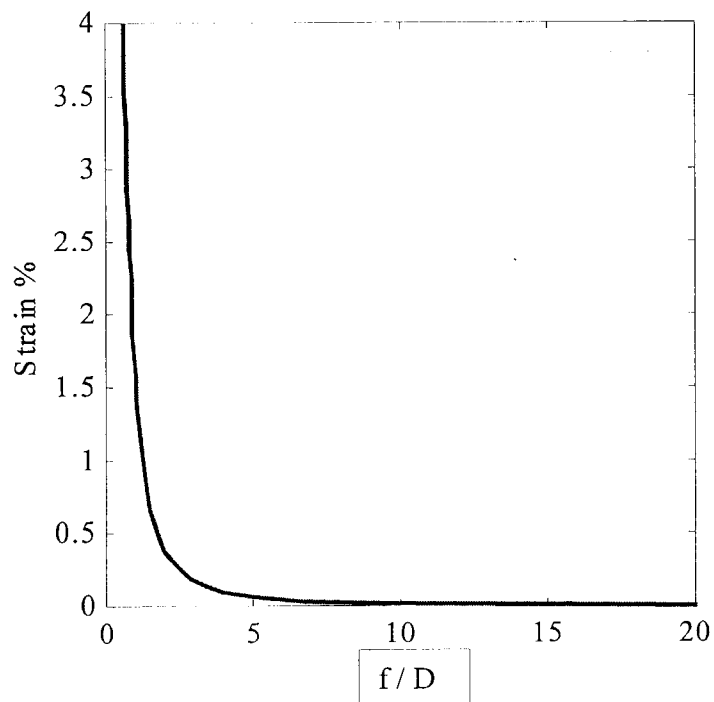


Required extension strain

$$S_{\max} = 4\%$$

CONTROLABILITY OF EAP MIRROR

- further investigation shows that the required maximum strain is a function of ar_1 i.e. a function of f-number
 - required maximum strain for desired mirror shape.



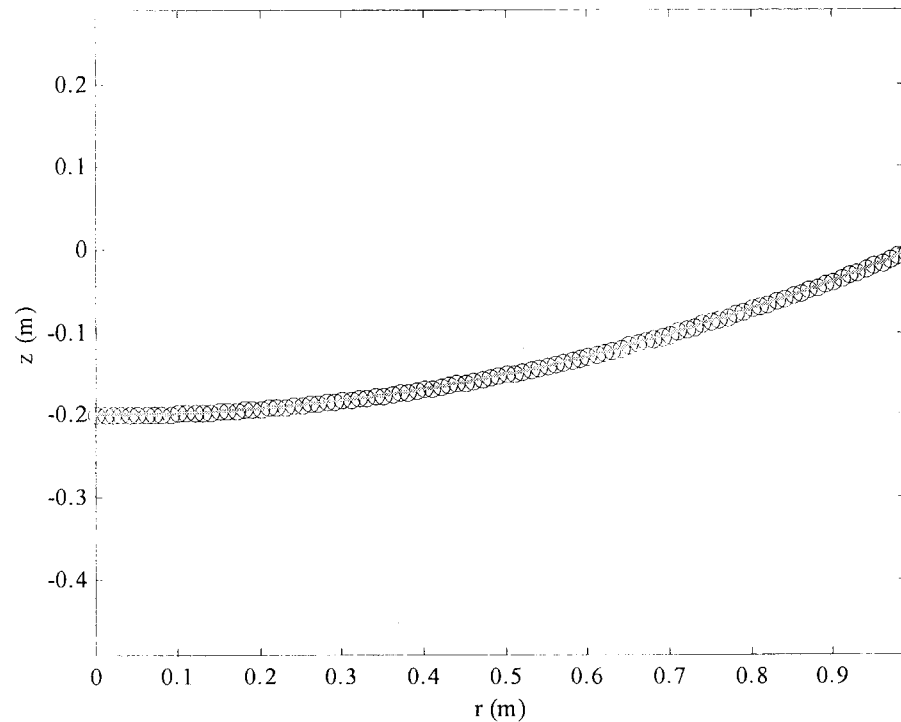
VERIFICATION BY FINITE ELEMENT

- 100 axisymmetric shell elements (Shell-151, ANSYS).
- Strain created by the electric field in the EAP films was simulated by thermal expansion.
- Large Deflection function of the ANSYS was activated.
- An artificial side pressure had been added first and was taken out after for final solution.

Table 1. Parameters used in FEM simulation

Film NO.	Diameter (m)	Thickness (μm)	E (Gpa)	Poisson's ratio σ
1	2	100	1	0.3
2	2	10	1	0.3

FEM RESULT



FEM results (blue circles) and parabolic curve fitting (green line)

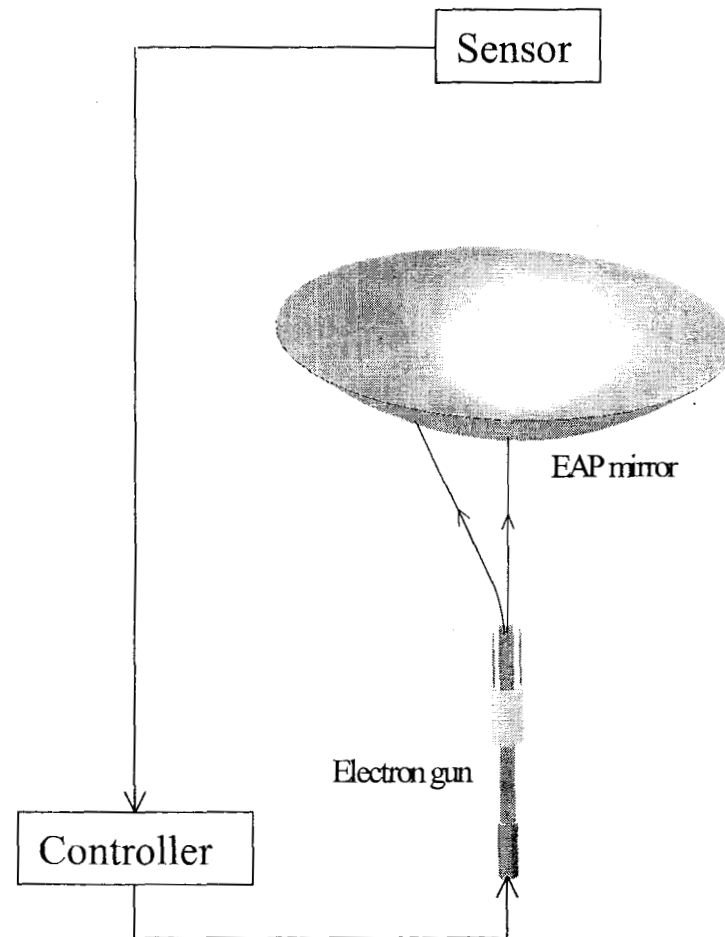
$$z = ar^2 + b$$

No difference between 10 and 100 μm films in this figure scale.

Concept of the Mirror System

Merits of the proposed concept

- **Simple uniform structure and wireless control** – simplify fabrication and control algorithm and easy to realize high precision.
- **Distributed control** – large number of equivalent controllable degree of freedom's that may be 10^6 per gun.
- **Compatible with inflatable optical technology** – help to reach desirable shape.



SUMMARY

	Completed work	On-going/future R&D
• USM	<ul style="list-style-type: none">• Prototype	<ul style="list-style-type: none">• Customized design• Explore control capability• Linear motor development
• USDC	<ul style="list-style-type: none">• Prototype• Sampling mechanisms• Demonstration of concept of deep coring, rock crush, etc	<ul style="list-style-type: none">• Rock sampler• Adapt it to meet various missions and R/D tasks• Operation at extreme environment• Lab on a drill
• EAP	<ul style="list-style-type: none">• Material characterization• Actuator demonstration• Analysis and concept of EAP mirror	<ul style="list-style-type: none">• Demonstrate controlled EAP mirror

ACKNOWLEDGMENT

To

- Current NDEAAer: Dr. Yoseph Bar-Cohen (team leader), Dr. Stewart Sherrit, Dr. Zensheu Chang and Dr. Shyh-Shiuh Lih
- Former NDEAAer: Dr. Ben Dolgin, Dr. José-María Sansiñena, Dr. Virginia Olazabal, Dr. Sean Leary and Dr. Tianji Xue
- Collaborators at Cybersonics Inc.: Dharmendra S. Pal, Shu Du, and Thomas Peterson
- Collaborators at QMI: Mr. Willem Grandia
- Co-op Students: Deborah Sigel, Mike Gradziel, Steve Askins
- Summer students worked at NDEAA
 - Ana Gjesdal, High School student, Summer 2000
 - Jose Rivera and Tao Stettler -- Summer Intern 2001
 - Lauren Wessel, SURF, and Sherman Hsu-Kuang Tu Summer, Intern, Summer 2003
- Dr. Greg Davis for his encouragement and help to this presentation.